Supporting Information

Supporting Information

Contents

List of Figures

List of Tables

List of Images

1. Experimental Details

Caution! Anhydrous HF, BF_3, GeF_4, AsF_5, and SbF_5 can cause severe burns and contact with the skin must be avoided and the compounds should only be handled in a well-ventilated fume hood. Any of the described formed salts may form HF by hydrolysis.

Materials and apparatus:

All reactions were carried out either in FEP/PFA reactors closed with a stainless steel valve, employing standard Schlenk technique with a stainless steel vacuum line. HF was dried with F_2 prior to use.

Raman spectra were recorded on a Bruker MultiRAM FT-Raman spectrometer with Nd:YAG laser excitation (λ = 1064 nm). For Raman measurements, samples of products were transferred into a cooled glass cell, which were evacuated afterwards. The educts were transferred into NMR tubes and measured at room temperature.

NMR spectra were recorded on a Jeol ECX400 NMR instrument. The spectrometer was externally referenced to $CFCl_3$ for ^{19}F, CH_3NO_2 for ^{14}N and to tetramethylsilane for ^{1}H and ^{13}C NMR spectra. The spectra were recorded inside 4 mm FEP NMR tube inliners. Acetone-d_6 was employed for external shimming when *a*HF was used as solvent for the respective compounds. The NMR samples were prepared by (re-)dissolving the respective compound at the designated measuring temperature in *a*HF and transferring the solution into a 4 mm FEP NMR tube inliner. The inliner was then frozen and flame sealed. For visualization and evaluation MestReNova Version 12.0.2 was employed.[1]

The low-temperature X-ray diffraction of was performed with an Oxford X-Calibur3 equipped with a Kappa CCD detector, operating with Mo-K_α radiation (λ = 0.71073 Å) and a Spellman generator (voltage 50 kV, current 40 mA). The program CrysAlisPro 1.171.38.46 (Rigaku OD, 2015)[2] was employed for the data collection and reduction. The structures were solved utilizing SHELXT[3] and SHELXL-2018/3[4] of the WINGX software package.[5] The structures were checked using the software PLATON.[6] The absorption correction was performed using the SCALE3 ABPSACK multiscan method.[7] Visualization was done by Mercury 2020.2.0.[8]

Computational methods:

All here presented calculations were done using DFT, B3LYP/6-311G++(3d2f,3p2d) level of theory by Gaussian 16.[9] NMR calculations were done using the GIAO method on the described level. Mapped Electrostatic Potentials were calculated using DFT, B3LYP/6-311G++(3df, 2pd) level of theory by Gaussian 09.[10]

Preparations:

Urazole was used without further purification. Urazole (98%) were purchased from abcr. Purity was checked by NMR and Raman spectroscopy.

Synthesis of $[C_2N_3H_3O(OH)][SbF_6]$:

Antimony pentafluoride (135 mg, 0.62 mmol, 1 eq.) and anhydrous HF (ca. 3 mL) were condensed into an FEP reactor at –196 °C. The mixture was homogenized at –40 °C for 15 min. After freezing the solution, urazole (63 mg, 0.62 mmol, 1 eq.) was added under nitrogen atmosphere. Followed by removing the nitrogen from the reaction vessel, the mixture was warmed to –40 °C and vigorously mixed. The mixture was then cooled down to –78°C, so that excess *a*HF could be removed from the system. $[C_2N_3H_3O(OH)][SbF_6]$ was obtained as a colorless solid, which was stable at room temperature over some hours.

Synthesis of $[C_2N_3H_3O(OH)][BF_3]$:

Boron trifluoride (68 mg, 1 mmol, 4 eq.) and anhydrous HF (ca. 3 mL) were condensed into an FEP reactor at –196 °C. The mixture was homogenized at –40 °C for 15 min. After freezing the solution, urazole (25 mg, 0.25 mmol, 1 eq.) was added under nitrogen atmosphere. Followed by removing the nitrogen from the reaction vessel, the mixture was warmed to –40 °C and vigorously mixed. The mixture was then cooled down to –78°C, so that excess *a*HF could be removed from the system. $[C_2N_3H_3O(OH)][BF_4]$ was obtained as a colorless solid, which was stable at room temperature over some minutes.

Synthesis of $[C_2N_3H_3(OH)_2][(SbF_6)_2]$:

Antimony pentafluoride (120 mg, 0.55 mmol, 3 eq.) and anhydrous HF (ca. 3 mL) were condensed into an FEP reactor at –196 °C. The mixture was homogenized at –40 °C for 15 min. After freezing the solution, urazole (19 mg, 0.18 mmol, 1 eq.) was added under

nitrogen atmosphere. Followed by removing the nitrogen from the reaction vessel, the mixture was warmed to –40 °C and vigorously mixed. The mixture was then cooled down to –78°C, so that excess *a*HF could be removed from the system. $[C_2N_3H_3O(OH)][SbF_6]$ was obtained as a colorless solid, which was stable at room temperature over some hours.

Synthesis of $[C_2N_3H_3(OH)_2][(AsF_6)_2]$:

Arsenic pentafluoride (204 mg, 1.2 mmol, 3 eq.) and anhydrous HF (ca. 3 mL) were condensed into an FEP reactor at –196 °C. The mixture was homogenized at –40 °C for 15 min. After freezing the solution, urazole (25 mg, 0.25 mmol, 1 eq.) was added under nitrogen atmosphere. Followed by removing the nitrogen from the reaction vessel, the mixture was warmed to –40 °C and vigorously mixed. The mixture was then cooled down to –78°C, so that excess *a*HF could be removed from the system. $[C_2N_3H_3(OH)_2][(AsF_6)_2]$ was obtained as a colorless solid, which was stable at room temperature over some minutes.

Synthesis of $[(C_2N_3H_3(OH))_2][Ge_2F_{10}]$:

Germanium tetrafluoride (178 mg, 1.2 mmol, 3 eq.) and anhydrous HF (ca. 3 mL) were condensed into an FEP reactor at –196 °C. The mixture was homogenized at –40 °C for 15 min. After freezing the solution, urazole (40 mg, 0.4 mmol, 1 eq.) was added under nitrogen atmosphere. Followed by removing the nitrogen from the reaction vessel, the mixture was warmed to –50 °C and vigorously mixed. The mixture was then cooled down to –78°C, so that excess *a*HF could be removed from the system. $[C_2N_3H_3(OH))_2][Ge_2F_{10}]$ was obtained as a colorless solid, which was stable at room temperature over some minutes.

2. Vibrational Data

2.1 Urazole and its protonated derivatives

Underlined numbers in the listings of the measured Raman frequencies indicate vibrations of the respective anions.

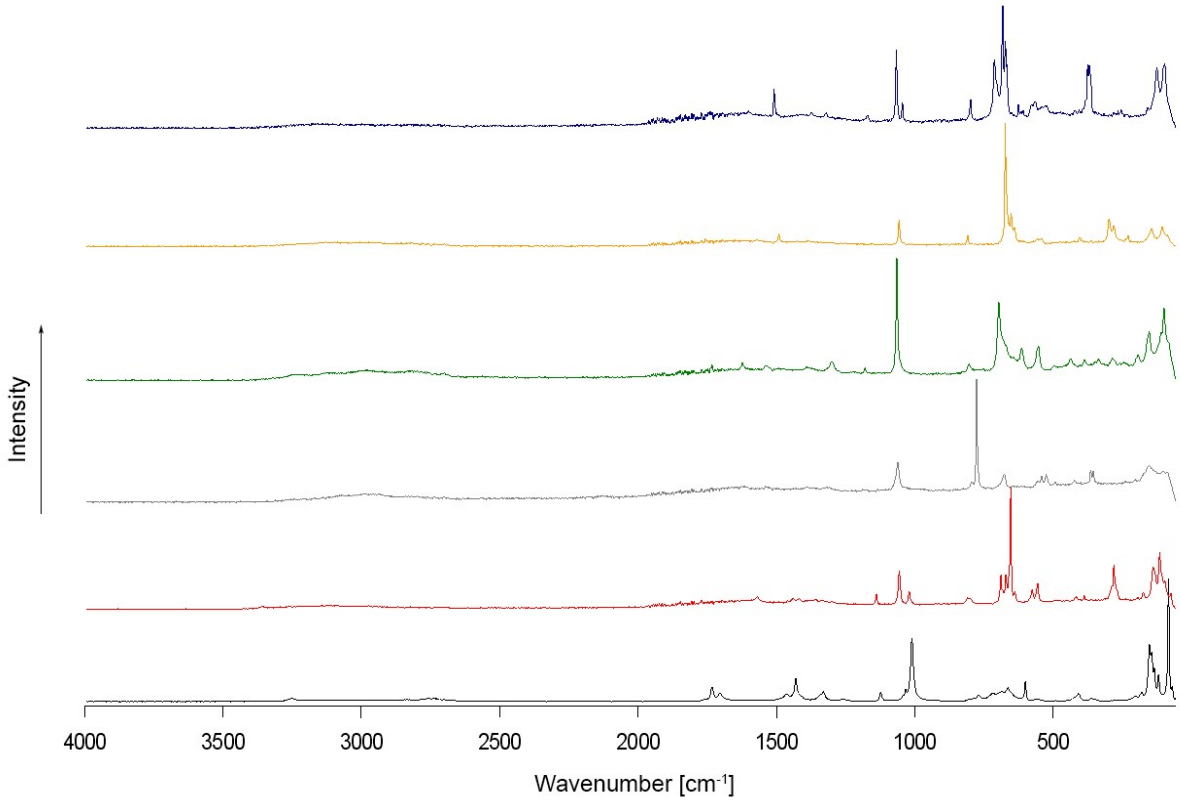

Figure 1: Raman spectra of urazole, $[C_2H_3N_3O(OH)][SbF_6]$, $[C_2H_3N_3O(OH)][BF_4]$, $[C_2H_3N_3(OH)_2][Ge_2F_{10}]$, $[C_2H_3N_3(OH)_2][(SbF_6)_2]$ and $[C_2H_3N_3(OH)_2][(AsF_6)_2]$.

Table 1: Observed vibrational frequencies and calculated vibrational frequencies of urazole [cm^{-1}] (calculated on B3LYP/6-311G++(3d2f, 3p2d) level of theory, Raman intensities in $Å^4/u$).

exp. frequency (Intensity)	calc. frequency (Intensity)	assignment
	3705(76)	ν (NH)
	3639(128)	ν (NH)
	3636(53)	ν (NH)
1733(12)	1755(27)	ν_s (CO)

1704(8)	1718(3)	ν_{as} (CO)
1464(6)		
1430(19)	1430(6)	ρ (NH)
	1405(5)	δ (NH)
1331(8)	1337(5)	δ (NH)
	1331(7)	δ (NH)
1258(2)	1205(6)	ν (CN)
1123(8)	1104(2)	ν (NN)
1043(5)		
1033(10)		
1010(52)	979(15)	ring breathing
770(6)	749(2)	δ (ring)
717(7)		
687(8)	704(2)	δ (ring) (out of plane)
664(11)	669(18)	τ (NH) + δ (ring)
601(17)		
558(2)	574(2)	δ (NH)
	555(3)	δ (NH)
	550(2)	δ (NH)
	518(3)	ω (NH)
409(7)		
362(3)	382(2)	δ (CO)
354(2)		
205(4)		
180(8)		
152(47)		
145(40)		
134(27)		
119(22)		
83(100)		
71(12)		
56(3)		

Table 2: Observed vibrational frequencies and calculated vibrational frequencies of $[C_2H_3N_3O(OH)][MF_y]$ [cm^{-1}] (M= Sb, B; y= 6 for Sb, y= 4 for B)(calculated on B3LYP/6-311G++(3d2f, 3p2d) level of theory, Raman intensities in $Å^4/u$).

exp. frequency (Intensity) [cation][SbF_6]	exp. frequency (Intensity) [cation][BF_4]	calc. frequency (Intensity)	assignment
		3755(119)	ν (OH)
		3648(126)	ν (NH)
		3638(31)	ν (NH)
		3633(18)	ν (NH)
		1810(20)	ν (CO)
	1625(14)	1669(3)	ν (CO(H))
1569(10)	1541(13)	1575(4)	ν (CN)
1440(9)		1430(5)	ρ (NH)
1420(9)			
1357(9)	1391(13)	1378(4)	δ (NH)
1332(7)	1315(13)	1320(2)	δ (NH)
1296(6)			
1139(13)		1140(5)	ν (C–N)
		1120(4)	ν (NN)
1056(31)	1061(33)	1085(11)	δ (OH)
1021(15)		1032(15)	ν (C–N)
		930(3)	ν (C–N)
809(10)			
800(9)	793(17)	760(3)	δ (CNN)
	777(100)		
689(28)		703(1)	δ (out-of-plane)
683(17)			
671(29)	677(23)	647(12)	ring breathing (CO)
654(100)			
638(15)		639(2)	δ (NH)
		633(2)	δ (NH) + δ (ring)
576(16)			
555(22)	559(17)	534(5)	δ (CO + COH)
	542(22)		
	526(23)		
	493(17)	475(3)	ω (NH + OH)

419(11)	422(18)		
388(12)	365(26)	391(2)	τ (NH + OH)
	355(26)		
		350(2)	δ (CO + COH)
		320(1)	δ (OH + NN)
288(20)		290(1)	δ (OH)
281(36)			
	240(18)		
194(10)	204(19)		
173(14)			
139(34)			
115(46)			
97(23)			
75(13)			

Table 3: Observed vibrational frequencies and calculated vibrational frequencies of $[C_2H_3N_3(OH)_2][MF_6]$ and $[C_2H_3N_3(OH)_2][Ge_2F_{10}]$ [cm^{-1}] (M= Sb, As)(calculated on B3LYP/6-311G++(3d2f, 3p2d) level of theory, Raman intensities in $Å^4/u$).

exp. frequency (Intensity) [cation][Ge_2F_{10}]	exp. frequency (Intensity) [cation][SbF_6][Sb_2F_{11}]	exp. frequency (Intensity) [cation][AsF_6]	calc. frequency (Intensity)	assignment
			3668(161)	ν (OH)
			3660(4)	ν (OH)
			3560(68)	ν (NH)
			3546(17)	ν (NH)
			3522(20)	ν (NH)
1733(13)			1719(1)	ν (CO)
1623(15)				
1535(12)	1570(6)	1508(32)	1528(4)	ν (CN)
	1492(10)		1493(11)	δ (NH)
1392(11)	1381(5)	1373(13)	1382(3)	δ (NH)
			1366(1)	δ (NH)
1300(16)		1320(13)	1311(5)	ν (CN) + δ (NH)

1180(10)		1170(11)	1139(2)	ν (NN)
1065(100)	1057(22) 1039(4)	1067(34) 1045(21)	1044(23)	ring breathing (CN)
			997(5)	δ (OH)
			992(3)	ν (OH)
800(12)	809(9)	798(24)	765(3)	δ (ring)
		713(56)		
697(64)	673(100)			
	652(27)	682(100)		
672(29)		673(71) 667(52)	666(16)	δ (2x COH, ring)
	639(15)	626(20)		
614(27)	616(5)	616(14)		
		609(15)		
		579(20)		
553(28)	557(7)	565(22)		
	541(7)	530(19)	523(4)	δ (OH + NH)
437(18)		422(15)		
	404(7)	407(15)	404(2)	$\omega + \tau$ (OH + NH)
		392(16)		
387(17)		383(24)	348(1)	δ (COH)
		375(52)		
		370(52)		
337(18)	298(23)			
287(18)	281(17)	281(14)		
	230(9)			
		254(15)		
192(21)				
153(40)	145(15)	159(17)		
110(39)	106(16)	126(49)		
100(60)		98(52)		
84(32)	87(10)			

3. Crystal structures

3.1 [$C_2N_3H_3O(OH)$][SbF_6]

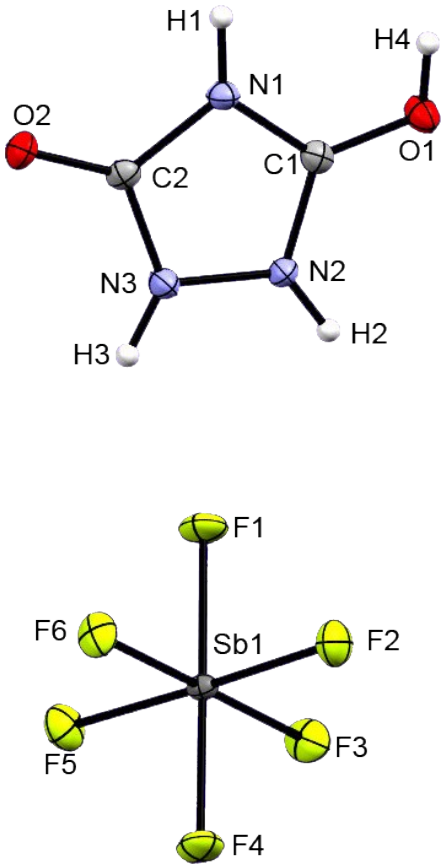

Figure 2: Asymmetric unit of [$C_2N_3H_3O(OH)$][SbF_6], view along *a*, displacement ellipsoids at 50% probability.

Monoprotonated Urazole crystallizes as [$C_2N_3H_3O(OH)$][SbF_6] in the monoclinic space group $P2_1/c$. A unit cell contains 4 formula units.

Table 4: Bond lengths (Å) of [$C_2N_3H_3O(OH)$][SbF_6].

Sb1	F3	1.8702(15)
Sb1	F5	1.8721(14)
Sb1	F2	1.8736(14)
Sb1	F4	1.8782(15)
Sb1	F1	1.8801(15)
Sb1	F6	1.8841(14)
O2	C2	1.233(3)
O1	C1	1.284(3)
N1	C1	1.347(3)
N1	C2	1.389(3)

N3	C2	1.342(3)
N3	N2	1.380(3)
N2	C1	1.315(3)

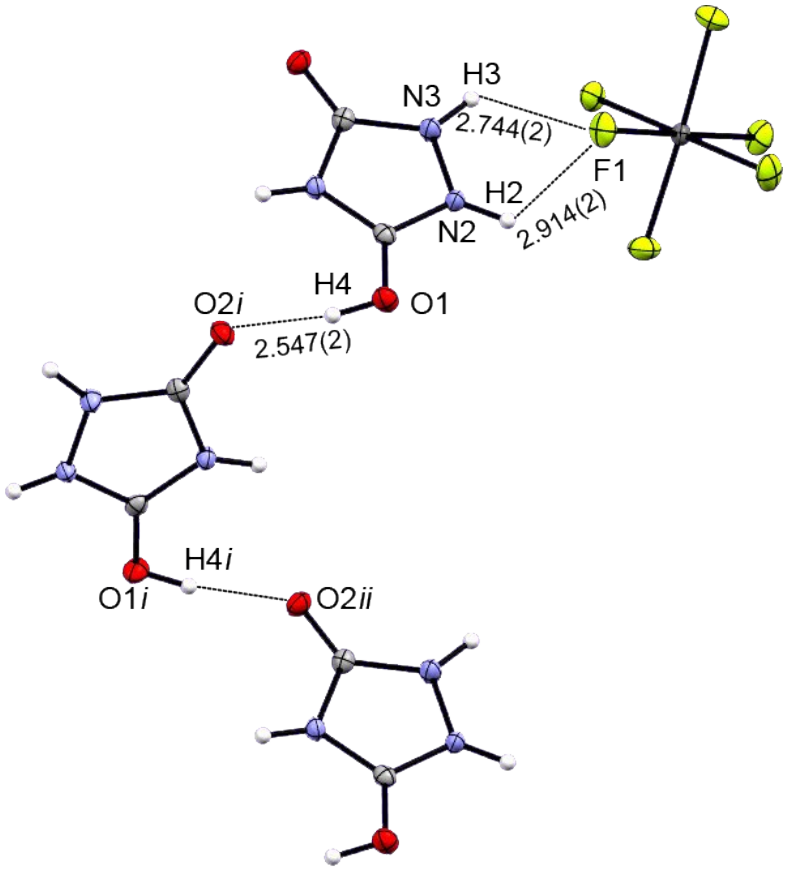

Figure 3: Cation-cation contacts in $[C_2N_3H_3O(OH)][SbF_6]$, view along *c*, displacement ellipsoids at 50% probability.

Table 5: Particular H-bond lengths (Å) for $[C_2N_3H_3O(OH)][SbF_6]$.

O2	O1`(via H4`)	2.547(2)

The cations are connected by hydrogen bonds between the protonated carbonyl group to the unprotonated carbonyl group of another cation, leading to endless zig-zag-chains.

Table 6: Data collection and structure refinement for $[C_2N_3H_3O(OH)][SbF_6]$.

	$[C_2N_3H_3O(OH)][SbF_6]$
Chemical formula	$C_2\ H_4\ F_6\ N_3\ O_2\ Sb$
Formula weight	337.84 g/mol
Temperature	110(2) K
Wavelength	0.71073 Å
Crystal size	0.195 x 0.141 x 0.106 mm
Crystal habit	colorless block
Crystal system	monoclinic
Space group	P $2_1/c$

Unit cell dimensions	a = 10.5271(9) Å	α = 90°
	b = 8.3036(4) Å	β = 118.384(11)°
	c = 10.5808(9) Å	γ = 90°
Volume	813.71(14) Å^3	
Z	4	
Density (calculated)	2.758 g/cm^3	
Absorption coefficient	3.480 mm^{-1}	
F(000)	632	
Diffractometer	Oxford XCalibur	
Radiation source	MoKα , λ = 0.71073 Å	
Index ranges	-13<=h<=15, -12<=k<=7, -15<=l<=13	
Reflections collected	2706	
Absorption correction	multi-scan	
Max. and min. transmission	1.000 and 0.797	
Structure solution program	SHELXT 2018/3 (Sheldrick, 2018)	
Refinement method	Full-matrix least-squares on F^2	
Refinement program	SHELXL-2018/3 (Sheldrick, 2018)	
Goodness-of-fit on F^2	1.043	
Final R indices	2378 data; I>2σ(I)	R1 = 0.0233, wR2 = 0.0515
	all data	R1 = 0.0295
Weighting scheme	w=1/[¥s^2^(Fo^2^)+(0.0204P)^2^] where P=(Fo^2^+2Fc^2^)/3	
Largest diff. peak and hole	1.162 and -0.731 eÅ^{-3}	
R.M.S. deviation from mean	0.137 eÅ^{-3}	
CCDC-deposition number	2072534	

Table 7: Bond angles (°) for $[C_2N_3H_3O(OH)][SbF_6]$.

F3	Sb1	F5	90.77(7)
F3	Sb1	F2	92.59(7)
F5	Sb1	F2	176.64(7)
F3	Sb1	F4	90.03(7)
F5	Sb1	F4	89.14(6)
F2	Sb1	F4	90.94(7)
F3	Sb1	F1	89.67(7)
F5	Sb1	F1	90.09(6)

F2	Sb1	F1	89.84(7)
F4	Sb1	F1	179.18(7)
F3	Sb1	F6	179.23(7)
F5	Sb1	F6	89.62(7)
F2	Sb1	F6	87.02(7)
F4	Sb1	F6	89.31(7)
F1	Sb1	F6	91.00(7)
C1	N1	C2	109.50(19)
C2	N3	N2	109.71(19)
C1	N2	N3	107.82(19)
O2	C2	N3	127.5(2)
O2	C2	N1	127.9(2)
N3	C2	N1	104.61(19)
O1	C1	N2	123.8(2)
O1	C1	N1	127.8(2)
N2	C1	N1	108.32(19)

Table 8: Anisotropic atomic displacement parameters ($Å^2$) for $[C_2N_3H_3O(OH)][SbF_6]$.

	U_{11}	U_{22}	U_{33}	U_{23}	U_{13}	U_{12}
Sb1	0.00913(8)	0.01250(8)	0.01016(8)	-0.00045(5)	0.00441(6)	-0.00041(5)
F4	0.0210(8)	0.0303(8)	0.0101(7)	-0.0003(6)	0.0022(6)	-0.0043(6)
F5	0.0278(8)	0.0164(7)	0.0259(8)	-0.0001(6)	0.0143(7)	0.0058(6)
F1	0.0187(8)	0.0309(8)	0.0102(7)	-0.0002(6)	0.0016(6)	-0.0007(6)
F6	0.0170(7)	0.0227(7)	0.0285(8)	0.0030(6)	0.0165(7)	-0.0005(6)
F2	0.0279(9)	0.0139(7)	0.0277(8)	-0.0013(6)	0.0120(7)	0.0010(6)
F3	0.0170(7)	0.0349(9)	0.0280(8)	0.0084(7)	0.0143(7)	-0.0018(6)
O2	0.0152(8)	0.0163(8)	0.0193(9)	0.0003(6)	0.0086(7)	-0.0037(6)
O1	0.0171(9)	0.0170(8)	0.0195(9)	0.0057(7)	0.0102(8)	0.0021(7)
N1	0.0098(9)	0.0150(9)	0.0126(9)	0.0014(7)	0.0038(8)	0.0008(7)
N3	0.0122(10	0.0155(10	0.0154(10	0.0043(7)	0.0052(8)	0.0001(7)

	)	)	)			
N2	0.0103(9)	0.0128(9)	0.0143(9)	0.0016(7)	0.0044(8)	-0.0012(7)
C2	0.0132(11)	0.0148(10)	0.0109(10)	-0.0014(8)	0.0061(9)	-0.0008(8)
C1	0.0137(11)	0.0125(9)	0.0124(10)	-0.0011(8)	0.0066(9)	0.0017(8)

3.2 $[C_2N_3H_3(OH)_2][Ge_2F_{10}]$

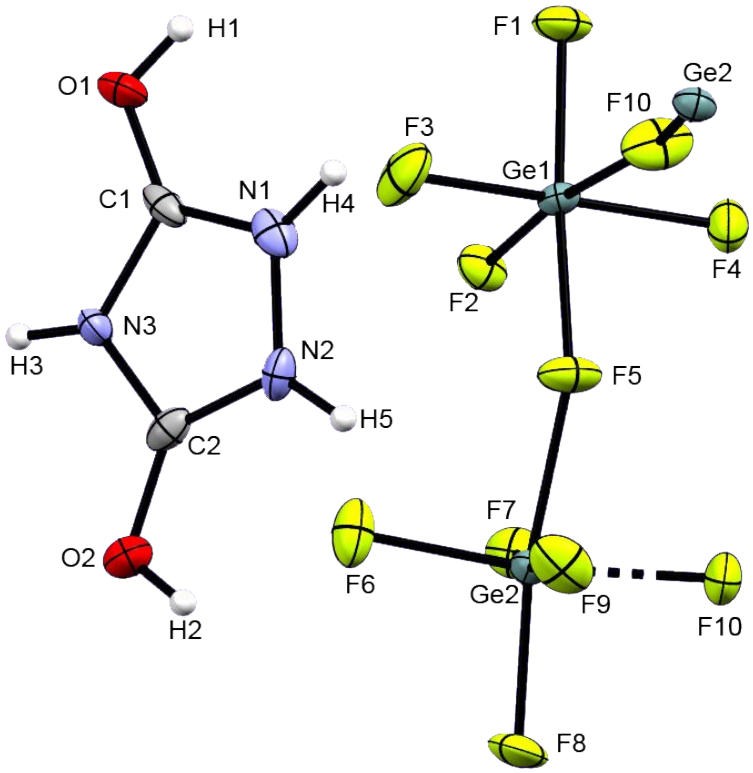

Figure 4: Asymmetric unit of $[C_2N_3H_3(OH)_2][Ge_2F_{10}]$, view along *a*, displacement ellipsoids at 50% probability.

Diprotonated Urazole crystallizes as $[C_2N_3H_3(OH)_2][Ge_2F_{10}]$ in the monoclinic space group $P2_1/n$. A unit cell contains 4 formula units.

Table 9: Bond lengths (Å) of $[C_2N_3H_3(OH)_2][Ge_2F_{10}]$.

Ge1	F3	1.714(3)
Ge1	F2	1.743(3)
Ge1	F4	1.757(3)
Ge1	F1	1.774(3)
Ge1	F5	1.870(3)

Ge1	F10	1.910(4)
Ge2	F6	1.730(4)
Ge2	F9	1.736(4)
Ge2	F7	1.755(3)
Ge2	F8	1.762(3)
Ge2	F10	1.893(3)
Ge2	F5	1.895(3)
O1	C1	1.277(7)
O1	H1	0.8200
O2	C2	1.289(7)
O2	H2	0.8201
N1	C1	1.313(8)
N1	N2	1.370(7)
N1	H4	0.8601
N2	C2	1.301(8)
N2	H5	0.8599
N3	C2	1.349(7)
N3	C1	1.360(7)
N3	H3	0.8600

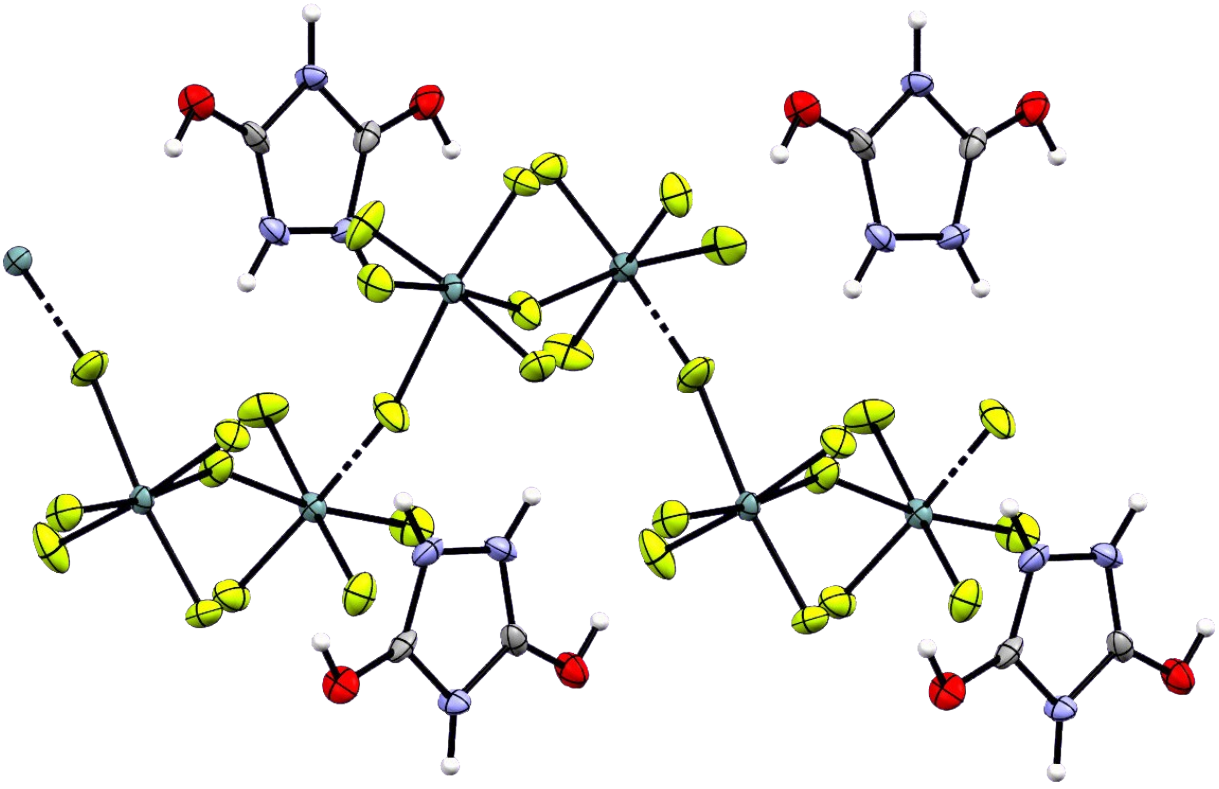

Figure 5: Packing of $[C_2N_3H_3(OH)_2][Ge_2F_{10}]$, view along *c*, displacement ellipsoids at 50% probability.

The cations are arranged around the infinite Ge_2F_{10} anion chain.

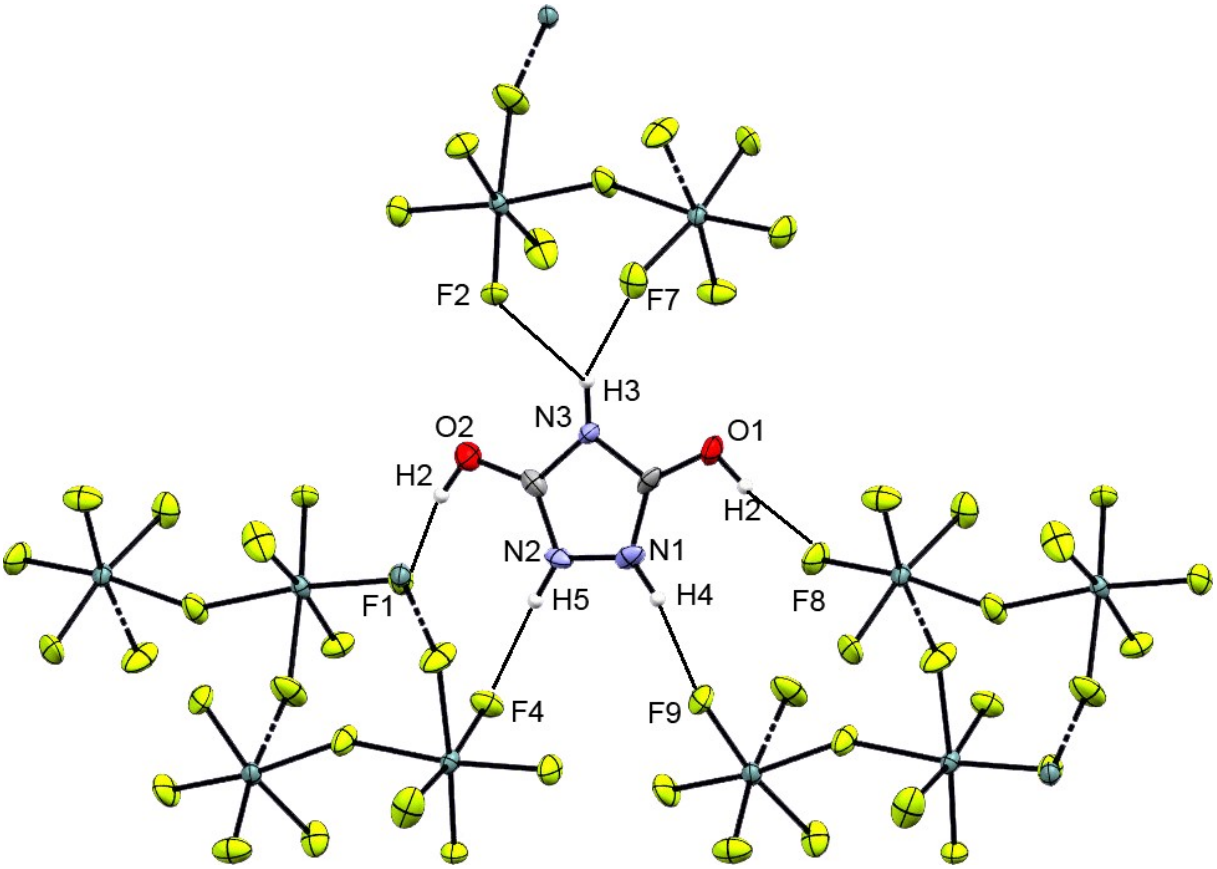

Figure 6: Particular hydrogen bonds of $[C_2N_3H_3(OH)_2][Ge_2F_{10}]$, view along *a*, displacement ellipsoids at 50% probability.

Table 10: Particular H-bond lengths (Å) for $[C_2N_3H_3(OH)_2][Ge_2F_{10}]$.

O2 (via H2)	F1	2.519(6)
O1 (via H1)	F8	2.531(6)
N2 (via H5)	F4	2.673(7)
N1 (via H4)	F9	2.616(7)
N3 (via H3)	F2	2.763(6)
N3 (via H3)	F7	2.976(6)

Compared to the monoprotonated species, no contacts between the cations can be detected. Each hydrogen atom exhibits strong to moderate hydrogen bonds to various $[Ge_2F_{10}]$ chains.

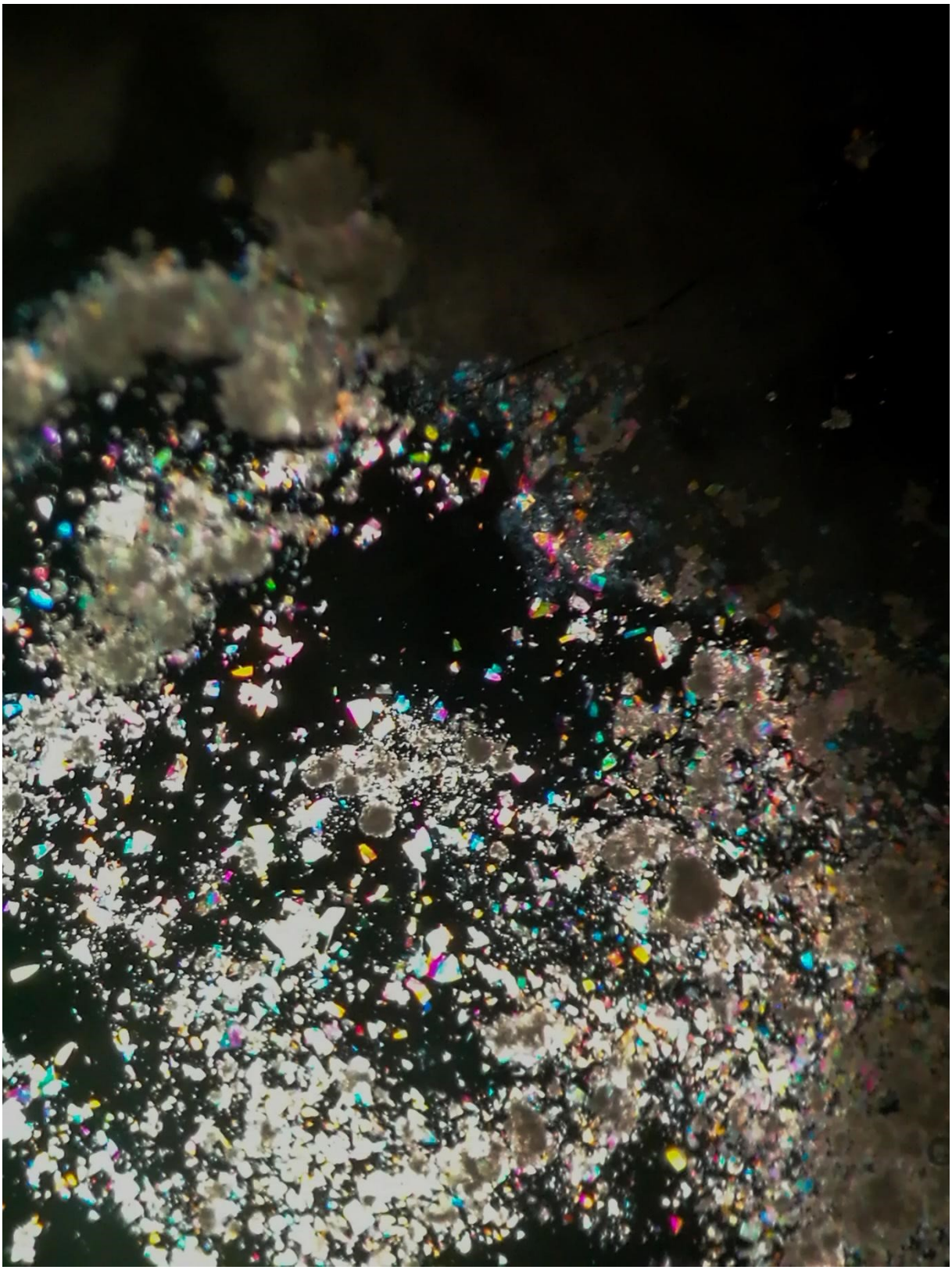

Image 1: Crystals of $[C_2N_3H_3(OH)_2][Ge_2F_{10}]$ under the microscope.

Table 11: Data collection and structure refinement for $[C_2N_3H_3(OH)_2][Ge_2F_{10}]$.

	$[C_2N_3H_3(OH)_2][Ge_2F_{10}]$	
Chemical formula	$C_2\ H_5\ F_{10}\ Ge_2\ N_3\ O_2$	
Formula weight	438.31 g/mol	
Temperature	101(2) K	
Wavelength	0.71073 Å	
Crystal size	0.395 x 0.268 x 0.212 mm	
Crystal habit	colorless plate	
Crystal system	monoclinic	
Space group	P $2_1/n$	
Unit cell dimensions	a = 7.8994(10) Å	α = 90°
	b = 18.299(3) Å	β = 114.751(16)°
	c = 8.1991(11) Å	γ = 90°
Volume	1076.3(3) $Å^3$	
Z	4	
Density (calculated)	2.705 g/cm^3	
Absorption coefficient	5.733 mm^{-1}	
F(000)	832	
Diffractometer	Oxford XCalibur	
Radiation source	MoKα , λ = 0.71073 Å	
Index ranges	-9<=h<=8, -22<=k<=19, -9<=l<=10	
Reflections collected	2194	
Absorption correction	multi-scan	
Max. and min. transmission	1.000 and 0.765	
Structure solution program	SHELXT 2018/3 (Sheldrick, 2018)	
Refinement method	Full-matrix least-squares on F^2	
Refinement program	SHELXL-2018/3 (Sheldrick, 2018)	
Goodness-of-fit on F^2	1.030	
Final R indices	1731 data; I>2σ(I)	R1 = 0.0471, wR2 = 0.1183
	all data	R1 = 0.0640
Weighting scheme	w=1/[¥s^2^(Fo^2^)+(0.0538P)^2^] where P=(Fo^2^+2Fc^2^)/3	
Largest diff. peak and hole	1.334 and -0.954 $eÅ^{-3}$	
R.M.S. deviation from mean	0.190 $eÅ^{-3}$	
CCDC-deposition number	2072535	

Table 12: Bond angles (°) for $[C_2N_3H_3(OH)_2][Ge_2F_{10}]$.

F3	Ge1	F2	94.42(18)
F3	Ge1	F4	172.38(19)
F2	Ge1	F4	92.33(16)
F3	Ge1	F1	92.19(17)
F2	Ge1	F1	95.98(16)
F4	Ge1	F1	90.60(16)
F3	Ge1	F5	88.07(17)
F2	Ge1	F5	91.63(16)
F4	Ge1	F5	88.22(16)
F1	Ge1	F5	172.34(17)
F3	Ge1	F10	89.71(19)
F2	Ge1	F10	172.80(15)
F4	Ge1	F10	83.22(16)
F1	Ge1	F10	89.74(16)
F5	Ge1	F10	82.61(16)
F6	Ge2	F9	94.02(17)
F6	Ge2	F7	91.07(17)
F9	Ge2	F7	171.41(18)
F6	Ge2	F8	97.85(18)
F9	Ge2	F8	92.31(18)
F7	Ge2	F8	93.85(17)
F6	Ge2	F10	171.55(17)
F9	Ge2	F10	88.82(18)
F7	Ge2	F10	85.20(18)
F8	Ge2	F10	89.98(17)
F6	Ge2	F5	90.57(17)
F9	Ge2	F5	84.63(16)
F7	Ge2	F5	88.41(15)
F8	Ge2	F5	171.24(18)
F10	Ge2	F5	81.77(15)

Ge1	F5	Ge2	149.0(2)
Ge2	F10	Ge1	160.5(2)
C1	O1	H1	110.2
C2	O2	H2	108.6
C1	N1	N2	108.2(5)
C1	N1	H4	125.6
N2	N1	H4	126.3
C2	N2	N1	108.2(5)
C2	N2	H5	125.8
N1	N2	H5	126.0
C2	N3	C1	107.7(6)
C2	N3	H3	126.6
C1	N3	H3	125.7
O1	C1	N1	130.1(6)
O1	C1	N3	122.4(6)
N1	C1	N3	107.5(5)
O2	C2	N2	129.1(6)
O2	C2	N3	122.5(6)
N2	C2	N3	108.4(5)

Table 13: Anisotropic atomic displacement parameters (Å^2) for $[C_2N_3H_3(OH)_2][Ge_2F_{10}]$.

	U_{11}	U_{22}	U_{33}	U_{23}	U_{13}	U_{12}
Ge1	0.0129(3)	0.0165(4)	0.0104(3)	-0.0017(3)	0.0035(2)	0.0005(2)
Ge2	0.0163(3)	0.0162(4)	0.0114(3)	-0.0001(3)	0.0060(2)	-0.0022(2)
F1	0.0324(19)	0.027(2)	0.0118(16)	-0.0001(16)	0.0029(14)	0.0037(16)
F2	0.0279(18)	0.015(2)	0.0208(17)	0.0016(15)	0.0103(14)	0.0053(15)
F3	0.0235(18)	0.049(3)	0.036(2)	-0.015(2)	0.0166(16)	-0.0181(19)
F4	0.0235(17)	0.021(2)	0.0304(19)	0.0031(17)	0.0099(14)	-0.0050(16)
F5	0.0293(17)	0.027(2)	0.0130(17)	-0.0027(15)	0.0026(13)	0.0087(17)
F6	0.0223(17)	0.020(2)	0.048(2)	-0.0019(19)	0.0183(16)	-0.0027(16)

F7	0.0196(17)	0.037(3)	0.0252(18)	0.0023(18)	0.0123(14)	0.0062(17)
F8	0.051(2)	0.030(2)	0.0114(17)	0.0067(17)	0.0021(16)	-0.002(2)
F9	0.047(2)	0.026(2)	0.0272(19)	-0.0018(18)	0.0252(16)	0.0087(19)
F10	0.0302(19)	0.028(2)	0.030(2)	-0.0049(18)	0.0048(15)	0.0156(18)
O1	0.030(2)	0.026(3)	0.0123(19)	0.0049(19)	0.0068(16)	-0.001(2)
O2	0.025(2)	0.025(3)	0.017(2)	-0.003(2)	0.0045(16)	-0.005(2)
N1	0.017(2)	0.018(3)	0.027(3)	0.007(2)	0.011(2)	0.007(2)
N2	0.020(2)	0.013(3)	0.026(3)	-0.005(2)	0.012(2)	-0.005(2)
N3	0.022(2)	0.013(3)	0.014(2)	0.003(2)	0.0072(19)	-0.001(2)
C1	0.016(3)	0.020(4)	0.020(3)	0.011(3)	0.009(2)	0.007(3)
C2	0.013(3)	0.021(4)	0.019(3)	-0.007(3)	0.007(2)	-0.002(2)

3.3 $[C_2N_3H_3(OH)_2][(AsF_6)_2]$

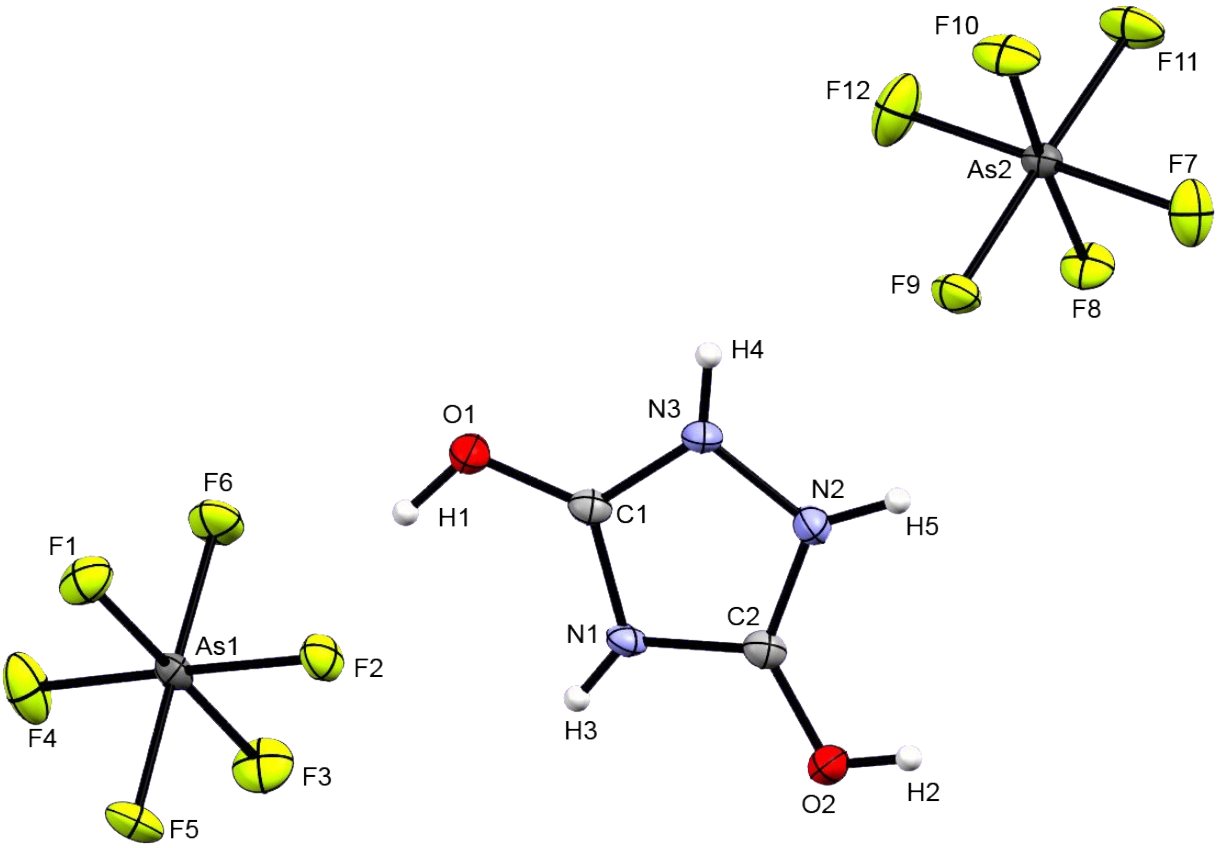

Figure 7: Asymmetric unit of $[C_2N_3H_3(OH)_2][(AsF_6)_2]$, view along *a*, displacement ellipsoids at 50% probability.

Diprotonated Urazole crystallizes as $[C_2N_3H_3(OH)_2][(AsF_6)_2]$ in the orthorhombic space group *P*bca. A unit cell contains 8 formula units.

Table 14: Bond lengths (Å) of $[C_2N_3H_3(OH)_2][(AsF_6)_2]$.

As1	F6	1.7074(16)
As1	F3	1.7074(18)
As1	F4	1.7084(19)
As1	F1	1.7165(17)
As1	F5	1.7355(16)
As1	F2	1.7444(17)
As2	F12	1.695(2)
As2	F10	1.7151(16)
As2	F9	1.7189(16)
As2	F8	1.7229(16)
As2	F11	1.7270(17)

As2	F7	1.7368(19)
O1	C1	1.279(4)
O2	C2	1.283(3)
N1	C2	1.354(4)
N1	C1	1.355(3)
N3	C1	1.308(4)
N3	N2	1.372(3)
N2	C2	1.316(3)

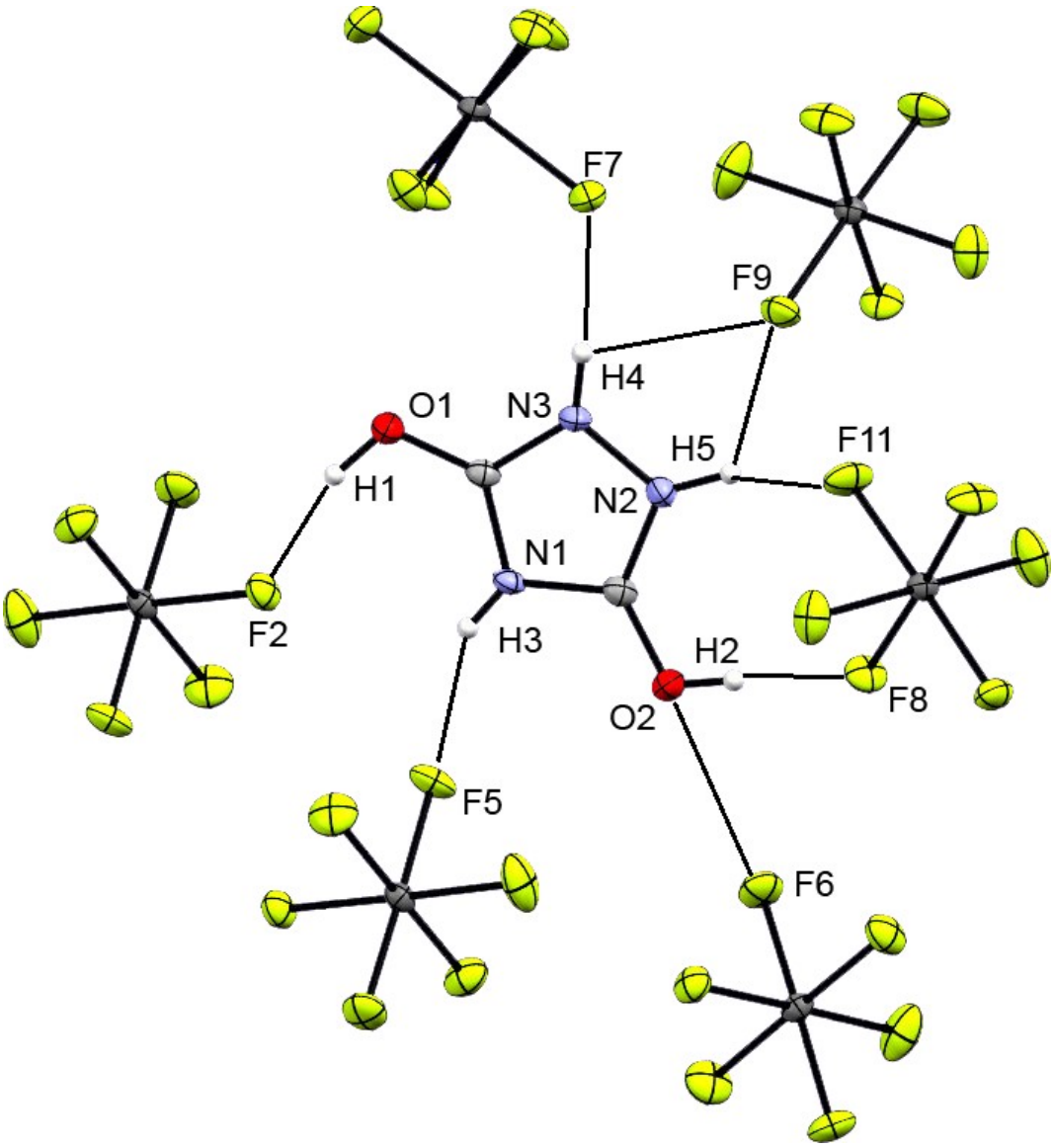

Figure 8: Particular hydrogen bonds of $[C_2N_3H_3(OH)_2][(AsF_6)_2]$, view along *c*, displacement ellipsoids at 50% probability.

Table 15: Particular H-bond lengths (Å) for $[C_2N_3H_3(OH)_2][(AsF_6)_2]$.

O1 (via H1)	F2	2.583(3)
O2 (via H2)	F6	2.791(3)
O2 (via H2)	F8	2.721(3)
N1 (via H3)	F5	2.722(3)
N2 (via H5)	F9	2.858(3)
N2 (via H5)	F11	2.768(3)
N3 (via H4)	F7	2.727(3)
N3 (via H4)	F9	2.858(3)

Table 16: Data collection and structure refinement for $[C_2N_3H_3(OH)_2][(AsF_6)_2]$.

	$[C_2N_3H_3(OH)_2][(AsF_6)_2]$	
Chemical formula	$C_2\ H_5\ As_2\ F_{12}\ N_3\ O_2$	
Formula weight	480.93 g/mol	
Temperature	108(2) K	
Wavelength	0.71073 Å	
Crystal size	0.540 x 0.233 x 0.143 mm	
Crystal habit	colorless plate	
Crystal system	orthorhombic	
Space group	Pbca	
Unit cell dimensions	a = 9.4694(7) Å	α = 90°
	b = 11.6800(7) Å	β = 90°
	c = 21.1896(11) Å	γ = 90°
Volume	2343.6(3) Å^3	
Z	8	
Density (calculated)	2.726 g/cm^3	
Absorption coefficient	5.874 mm^{-1}	
F(000)	1824	
Diffractometer	Oxford XCalibur	
Radiation source	MoKα , λ = 0.71073 Å	
Index ranges	-13<=h<=13, -17<=k<=13, -31<=l<=31	
Reflections collected	4001	
Absorption correction	multi-scan	
Max. and min. transmission	1.000 and 0.237	
Structure solution program	SHELXT 2018/3 (Sheldrick, 2018)	
Refinement method	Full-matrix least-squares on F^2	
Refinement program	SHELXL-2018/3 (Sheldrick, 2018)	

Goodness-of-fit on F^2	1.096	
Final R indices	3215 data; I>2 σ (I)	R1 = 0.0328, wR2 = 0.0735
	all data	R1 = 0.0489
Weighting scheme	w=1/[¥s^2^(Fo^2^)+(0.0260P)^2^+3.4141P] where P=(Fo^2^+2Fc^2^)/3	
Largest diff. peak and hole	1.020 and -0.846 eÅ^{-3}	
R.M.S. deviation from mean	0.144 eÅ^{-3}	
CCDC-deposition number	2072533	

Table 17: Bond angles (°) for $[C_2N_3H_3(OH)_2][(AsF_6)_2]$.

F6	As1	F3	90.67(9)
F6	As1	F4	91.41(10)
F3	As1	F4	90.31(10)
F6	As1	F1	90.83(9)
F3	As1	F1	178.19(9)
F4	As1	F1	90.67(10)
F6	As1	F5	178.53(9)
F3	As1	F5	89.53(9)
F4	As1	F5	90.04(9)
F1	As1	F5	88.95(8)
F6	As1	F2	90.16(9)
F3	As1	F2	90.20(9)
F4	As1	F2	178.35(9)
F1	As1	F2	88.78(9)
F5	As1	F2	88.39(8)
F12	As2	F10	91.43(10)
F12	As2	F9	91.26(10)
F10	As2	F9	90.27(8)
F12	As2	F8	91.76(9)
F10	As2	F8	176.63(10)
F9	As2	F8	90.76(8)
F12	As2	F11	90.38(11)
F10	As2	F11	89.52(8)
F9	As2	F11	178.35(10

			)
F8	As2	F11	89.35(8)
F12	As2	F7	179.77(12)
F10	As2	F7	88.67(10)
F9	As2	F7	88.53(9)
F8	As2	F7	88.15(9)
F11	As2	F7	89.83(10)
C2	N1	C1	107.9(2)
C1	N3	N2	108.4(2)
C2	N2	N3	108.0(2)
O1	C1	N3	123.5(2)
O1	C1	N1	128.6(3)
N3	C1	N1	107.9(3)
O2	C2	N2	130.2(3)
O2	C2	N1	122.0(2)
N2	C2	N1	107.8(2)

Table 18: Anisotropic atomic displacement parameters ($Å^2$) for $[C_2N_3H_3(OH)_2][(AsF_6)_2]$.

	U_{11}	U_{22}	U_{33}	U_{23}	U_{13}	U_{12}
As1	0.01570(15)	0.01354(12)	0.01227(12)	0.00120(9)	0.00223(9)	0.00198(10)
As2	0.01630(15)	0.01212(12)	0.01034(11)	0.00062(8)	-0.00090(9)	0.00127(10)
F9	0.0244(10)	0.0198(8)	0.0240(8)	-0.0062(6)	-0.0040(7)	0.0080(7)
F2	0.0197(10)	0.0229(8)	0.0201(8)	0.0005(6)	0.0067(7)	-0.0005(7)
F5	0.0337(11)	0.0156(8)	0.0183(8)	-0.0009(6)	0.0066(7)	0.0075(7)
F8	0.0281(11)	0.0272(9)	0.0109(7)	0.0008(6)	-0.0040(7)	0.0008(7)
F1	0.0268(11)	0.0235(8)	0.0247(8)	0.0008(7)	-0.0103(7)	-0.0004(7)
F7	0.0203(10)	0.0327(10)	0.0279(9)	0.0148(7)	0.0027(7)	-0.0013(8)
F11	0.0401(13)	0.0195(8)	0.0256(9)	-0.0037(7)	-0.0084(8)	0.0151(8)
F10	0.0436(13)	0.0256(9)	0.0131(7)	-0.0039(6)	-0.0103(7)	0.0104(8)
F6	0.0301(11)	0.0137(7)	0.0318(9)	0.0004(6)	0.0011(8)	0.0040(7)
F3	0.0358(13)	0.0353(10)	0.0166(8)	0.0022(7)	-0.0071(8)	0.0008(9)
F4	0.0252(12)	0.0331(10)	0.0396(11)	0.0161(8)	0.0161(8)	0.0042(8)
O1	0.0168(11)	0.0252(10)	0.0189(9)	-0.0059(8)	0.0018(8)	-0.0023(8)

F12	0.0248(12)	0.0358(10)	0.0409(11)	0.0158(9)	-0.0060(9)	-0.0127(8)
O2	0.0182(12)	0.0224(10)	0.0227(10)	-0.0069(8)	0.0024(8)	-0.0050(8)
N1	0.0171(12)	0.0142(10)	0.0112(9)	-0.0025(8)	0.0040(8)	0.0003(9)
N3	0.0164(13)	0.0183(11)	0.0147(10)	-0.0062(8)	0.0003(8)	0.0004(9)
N2	0.0141(13)	0.0210(11)	0.0165(10)	-0.0032(8)	0.0012(9)	0.0014(9)
C1	0.0191(14)	0.0144(11)	0.0101(10)	0.0001(8)	0.0013(9)	0.0004(10)
C2	0.0190(15)	0.0146(11)	0.0119(10)	0.0010(9)	0.0019(9)	-0.0001(10)

3.4 $[C_2N_3H_3(OH)_2][(SbF_6)_2] \cdot 2HF$

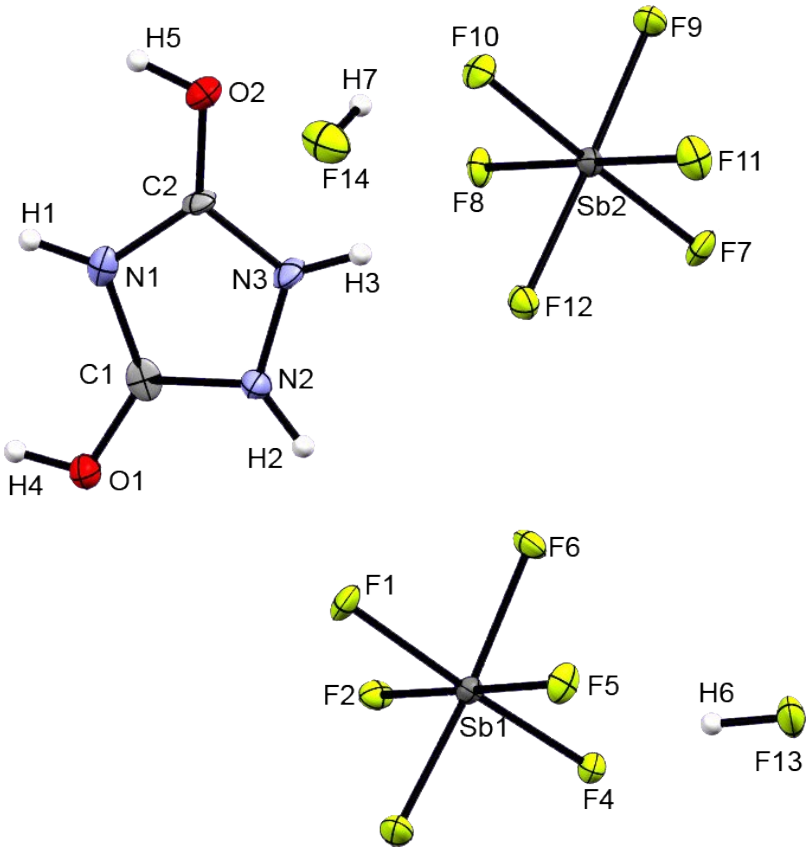

Figure 9: Asymmetric unit of $[C_2N_3H_3(OH)_2][(SbF_6)_2] \cdot 2HF$, view along *a*, displacement ellipsoids at 50% probability.

Diprotonated Urazole crystallizes as $[C_2N_3H_3(OH)_2][(SbF_6)_2] \cdot 2HF$ in the monoclinic space group *P*n. A unit cell contains 2 formula units.

Table 19: Bond lengths (Å) of $[C_2N_3H_3(OH)_2][(SbF_6)_2] \cdot 2HF$.

C2	O2	1.273(13)
C2	N3	1.294(14)
C2	N1	1.372(14)
N3	N2	1.373(8)
C1	O1	1.290(14)
C1	N2	1.296(15)
C1	N1	1.376(14)
Sb1	F4	1.849(11)
Sb1	F6	1.858(11)
Sb1	F5	1.876(7)
Sb1	F3	1.878(11)

Sb1	F2	1.899(6)
Sb1	F1	1.906(11)
Sb2	F9	1.857(11)
Sb2	F11	1.858(7)
Sb2	F7	1.877(12)
Sb2	F12	1.879(12)
Sb2	F8	1.880(6)
Sb2	F10	1.904(11)

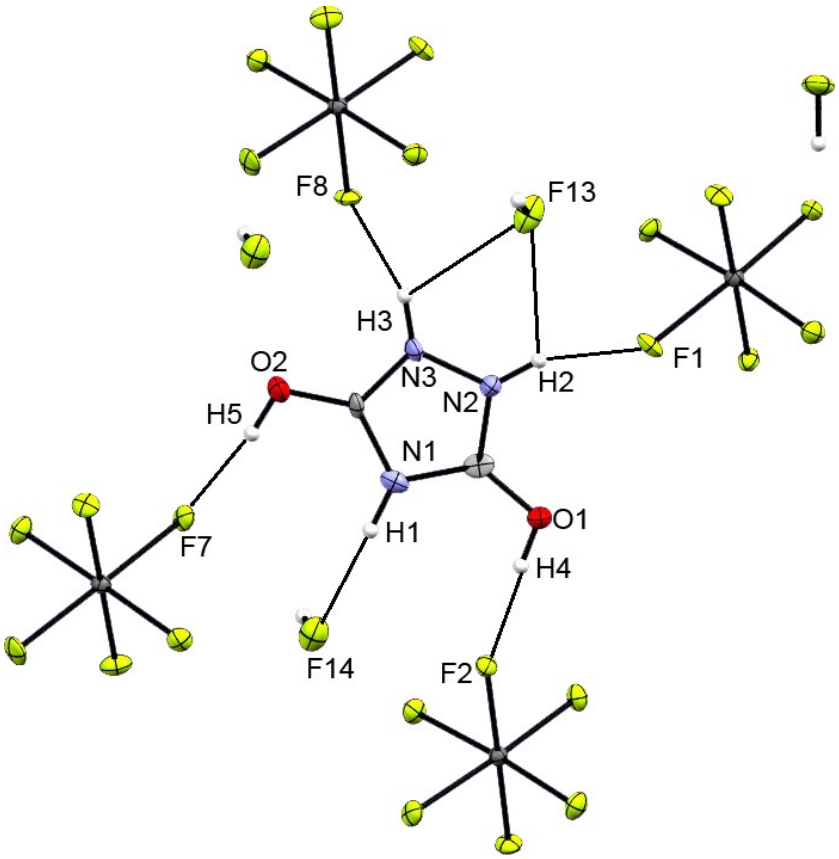

Figure 10: Particular hydrogen bonds of $[C_2N_3H_3(OH)_2][(SbF_6)_2] \cdot 2HF$, view along *c*, displacement ellipsoids at 50% probability.

Table 20: Particular H-bond lengths (Å) for $[C_2N_3H_3(OH)_2][(SbF_6)_2] \cdot 2HF$.

O1 (via H4)	F2	2.57(1)
O2 (via H5)	F7	2.59(1)
N1 (via H1)	F14	2.87(1)
N2 (via H2)	F1	2.66(1)
N2 (via H2)	F13	2.95(1)
N3 (via H3)	F8	2.71(1)

N3 (via H3)	F13	2.96(1)

Table 21: Data collection and structure refinement for $[C_2N_3H_3(OH)_2][(SbF_6)_2] \cdot 2HF$.

	$[C_2N_3H_3(OH)_2][SbF_6] \cdot 2HF$	
Chemical formula	$C_2\ H_7\ F_{14}\ N_3\ O_2\ Sb_2$	
Formula weight	614.63 g/mol	
Temperature	107(2) K	
Wavelength	0.71073 Å	
Crystal size	0.327 x 0.213 x 0.129 mm	
Crystal habit	colorless block	
Crystal system	monoclinic	
Space group	P n	
Unit cell dimensions	a = 6.5268(4) Å	α = 90°
	b = 8.4200(5) Å	β = 102.487(7)°
	c = 12.0682(8) Å	γ = 90°
Volume	647.53(7) $Å^3$	
Z	2	
Density (calculated)	3.512 g/cm^3	
Absorption coefficient	4.359 mm^{-1}	
F(000)	568	
Diffractometer	Oxford XCalibur	
Radiation source	MoK α , λ = 0.71073 Å	
Index ranges	-9<=h<=9, -12<=k<=12, -17<=l<=18	
Reflections collected	4344	
Absorption correction	multi-scan	
Max. and min. transmission	1.000 and 0.502	
Structure solution program	SHELXT 2018/3 (Sheldrick, 2018)	
Refinement method	Full-matrix least-squares on F^2	
Refinement program	SHELXL-2018/3 (Sheldrick, 2018)	
Goodness-of-fit on F^2	1.044	
Final R indices	3585 data; I>2 σ (I)	R1 = 0.0288, wR2 = 0.0568
	all data	R1 = 0.0410
Weighting scheme	w=1/[¥s^2^(Fo^2^)+(0.0175P)^2^] where P=(Fo^2^+2Fc^2^)/3	
Largest diff. peak and hole	1.121 and -0.843 $eÅ^{-3}$	

R.M.S. deviation from mean	0.178 eÅ^{-3}
CCDC-deposition number	2072532

Table 22: Bond angles (°) for $[C_2N_3H_3(OH)_2][(SbF_6)_2] \cdot 2HF$.

O2	C2	N3	123.9(11)
O2	C2	N1	128.4(11)
N3	C2	N1	107.6(9)
C2	N3	N2	110.0(8)
O1	C1	N2	122.1(11)
O1	C1	N1	128.6(12)
N2	C1	N1	109.3(10)
C1	N2	N3	107.0(8)
C2	N1	C1	106.0(10)
F4	Sb1	F6	90.5(5)
F4	Sb1	F5	89.2(4)
F6	Sb1	F5	89.4(4)
F4	Sb1	F3	94.4(5)
F6	Sb1	F3	175.1(6)
F5	Sb1	F3	91.0(4)
F4	Sb1	F2	90.5(5)
F6	Sb1	F2	89.4(5)
F5	Sb1	F2	178.8(7)
F3	Sb1	F2	90.2(5)
F4	Sb1	F1	176.9(6)
F6	Sb1	F1	86.5(5)
F5	Sb1	F1	91.1(4)
F3	Sb1	F1	88.6(5)
F2	Sb1	F1	89.0(5)
F9	Sb2	F11	91.8(4)
F9	Sb2	F7	89.8(5)
F11	Sb2	F7	90.4(4)
F9	Sb2	F12	178.2(6)
F11	Sb2	F12	89.1(4)
F7	Sb2	F12	91.8(5)
F9	Sb2	F8	89.4(5)
F11	Sb2	F8	178.2(6)

F7	Sb2	F8	90.9(5)
F12	Sb2	F8	89.7(5)
F9	Sb2	F10	88.8(5)
F11	Sb2	F10	88.9(4)
F7	Sb2	F10	178.5(6)
F12	Sb2	F10	89.6(5)
F8	Sb2	F10	89.7(5)

Table 23: Anisotropic atomic displacement parameters (Å^2) for $[C_2N_3H_3(OH)_2][(SbF_6)_2] \cdot 2HF$.

	U_{11}	U_{22}	U_{33}	U_{23}	U_{13}	U_{12}
C2	0.009(5)	0.020(6)	0.009(5)	-0.002(4)	-0.002(4)	0.000(4)
N3	0.014(3)	0.017(3)	0.012(3)	0.001(2)	-0.004(3)	-0.001(2)
C1	0.024(7)	0.007(4)	0.015(6)	-0.006(4)	0.010(5)	0.002(4)
N2	0.013(3)	0.014(3)	0.016(3)	0.002(2)	0.001(3)	-0.002(2)
N1	0.021(4)	0.013(3)	0.011(3)	0.000(3)	0.005(3)	0.005(3)
O1	0.017(3)	0.016(3)	0.018(3)	0.004(2)	0.002(2)	-0.002(2)
O2	0.015(3)	0.025(3)	0.016(3)	0.003(2)	-0.001(2)	0.000(2)
Sb1	0.0105(4)	0.0104(4)	0.0100(4)	0.0000(4)	0.0020(3)	0.0001(4)
F1	0.0174(11)	0.0181(11)	0.0113(10)	0.004(3)	-0.0007(9)	0.007(3)
F2	0.012(4)	0.011(4)	0.017(4)	-0.001(4)	0.002(3)	-0.001(4)
F3	0.0131(10)	0.0196(11)	0.0180(12)	0.004(3)	0.0067(9)	0.003(3)
F4	0.013(3)	0.017(3)	0.012(4)	0.004(3)	0.001(3)	-0.001(2)
F5	0.022(4)	0.007(3)	0.017(4)	0.000(4)	0.002(3)	0.003(4)
F6	0.012(4)	0.019(4)	0.016(4)	0.000(2)	0.007(3)	-0.003(3)
Sb2	0.0113(4)	0.0093(4)	0.0102(4)	-0.0002(4)	0.0023(3)	-0.0004(4)
F7	0.0174(11)	0.0181(11)	0.0113(10)	0.004(3)	-0.0007(9)	0.007(3)
F8	0.021(4)	0.008(4)	0.016(5)	0.004(3)	0.004(4)	-0.001(4)
F9	0.0131(10)	0.0196(11)	0.0180(12)	0.004(3)	0.0067(9)	0.003(3)
F10	0.016(4)	0.030(4)	0.007(4)	0.000(3)	-0.002(3)	-0.002(3)
F11	0.026(5)	0.012(3)	0.020(4)	-0.001(5)	0.010(4)	0.001(5)
F12	0.016(4)	0.017(4)	0.013(3)	0.001(2)	0.005(3)	-0.001(3)

F13	0.023(4)	0.028(3)	0.026(4)	0.016(3)	0.012(3)	0.006(3)
F14	0.024(4)	0.035(4)	0.021(3)	-0.008(3)	0.008(3)	-0.006(3)

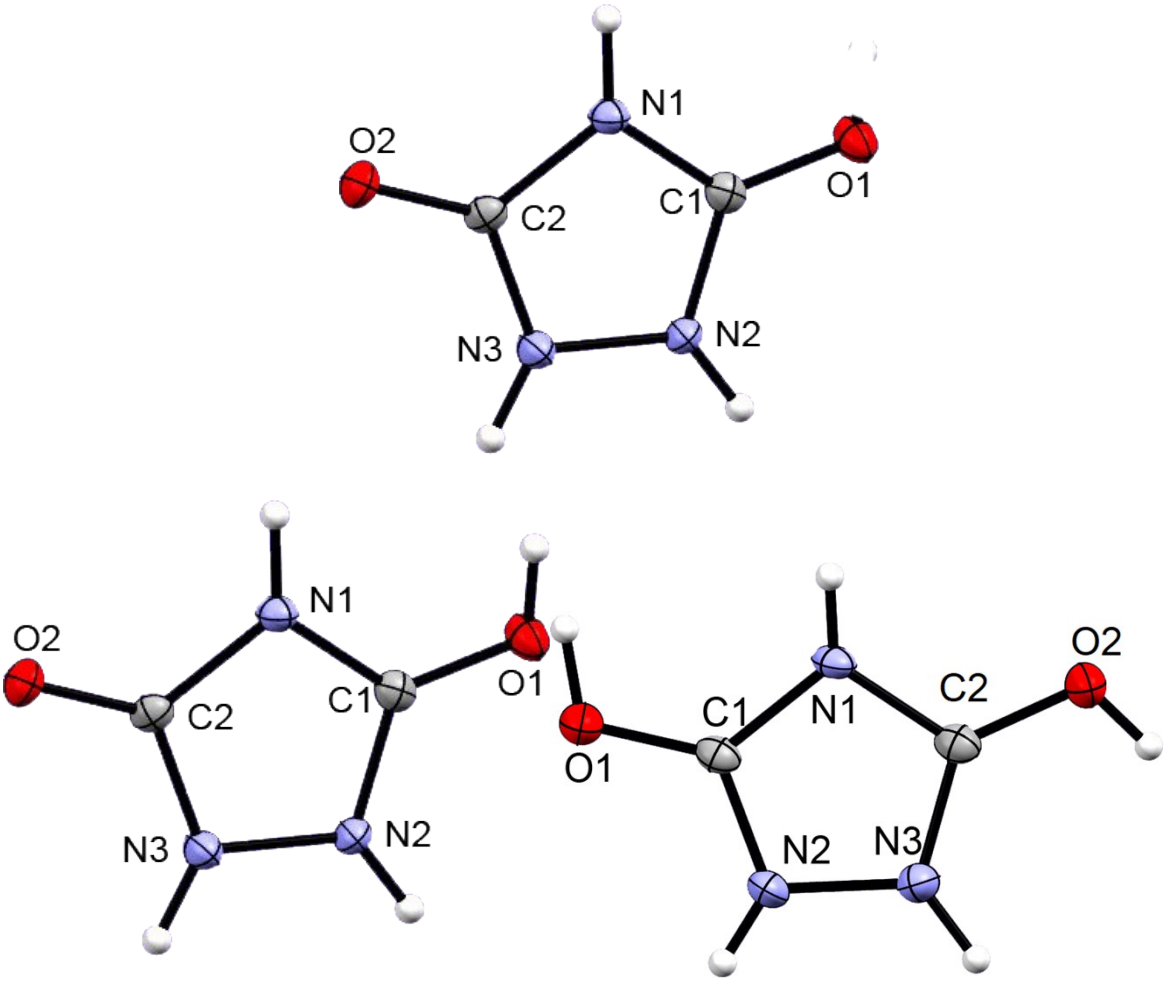

Table 24: Comparison of bond lengths (Å) of urazole, $[C_2N_3H_3O(OH)]$ and $[(C_2N_3H_3(OH)_2]$.

$C_2N_3H_3O_2$[11]			$[C_2N_3H_3O(OH)]$			$[C_2N_3H_3(OH)_2]$		
O2	C2	1.237(1)	O2	C2	1.233(3)	O2	C2	1.282(3)
O1	C1	1.232(1)	O1	C1	1.284(3)	O1	C1	1.278(3)
N1	C1	1.378(1)	N1	C1	1.347(3)	N1	C1	1.355(3)
N1	C2	1.380(1)	N1	C2	1.389(3)	N1	C2	1.354(4)
N3	C2	1.354(1)	N3	C2	1.342(3)	N3	C2	1.316(3)
N2	C1	1.367(1)	N2	C1	1.315(3)	N2	C1	1.308(4)
N3	N2	1.410(1)	N3	N2	1.380(3)	N3	N2	1.372(4)

4. NMR data

4.1 Urazole

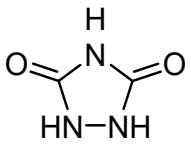

NMR (*a*HF, 20 °C) (ppm): $\delta(^{1}H) = 5.33$ (N-H); $\delta(^{14}N) = -244.69$; $\delta(^{13}C) = 151.75$.

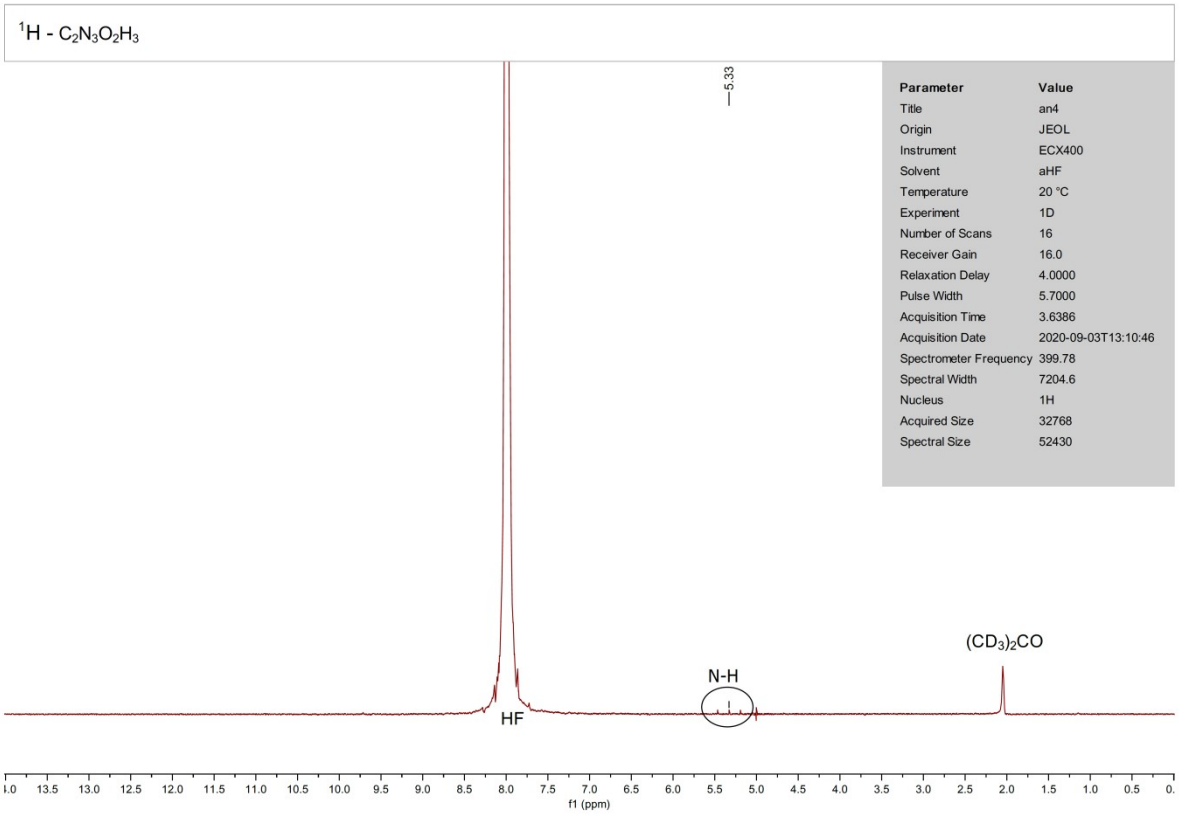

^{14}N - $C_2N_3O_2H_3$

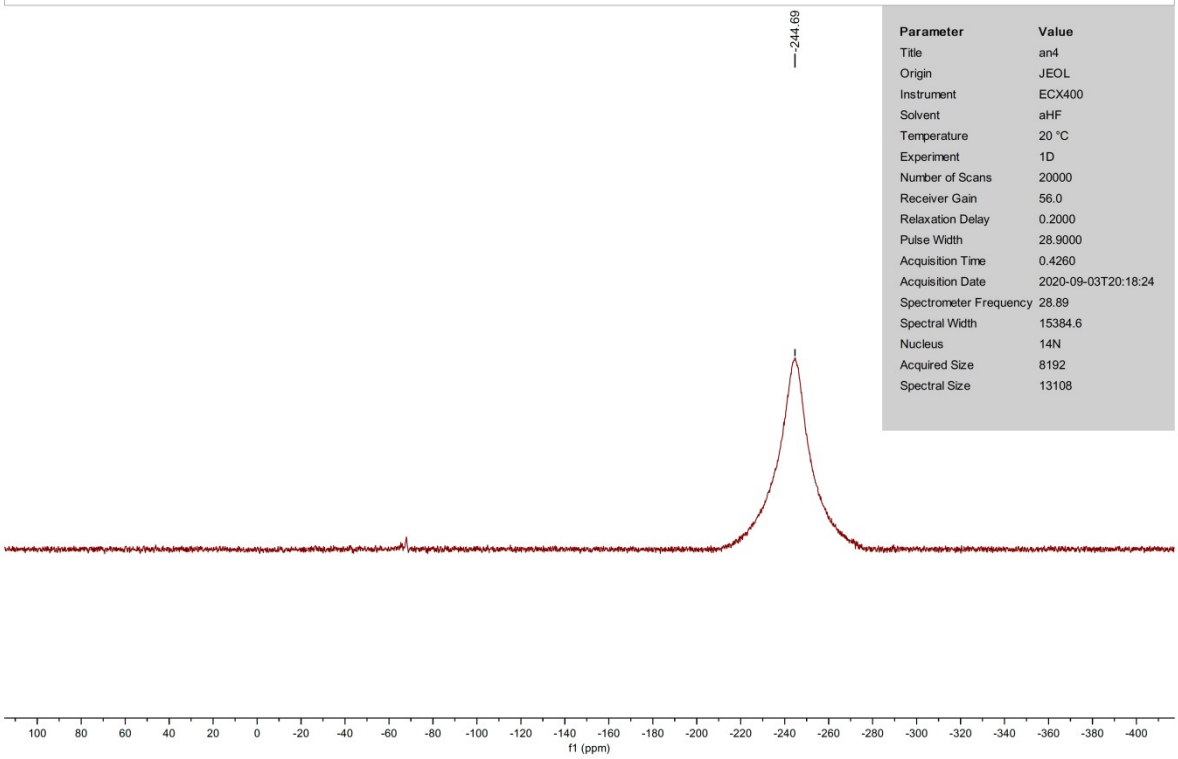

Parameter	Value
Title	an4
Origin	JEOL
Instrument	ECX400
Solvent	aHF
Temperature	20 °C
Experiment	1D
Number of Scans	20000
Receiver Gain	56.0
Relaxation Delay	0.2000
Pulse Width	28.9000
Acquisition Time	0.4260
Acquisition Date	2020-09-03T20:18:24
Spectrometer Frequency	28.89
Spectral Width	15384.6
Nucleus	14N
Acquired Size	8192
Spectral Size	13108

^{13}C - $C_2N_3O_2H_3$

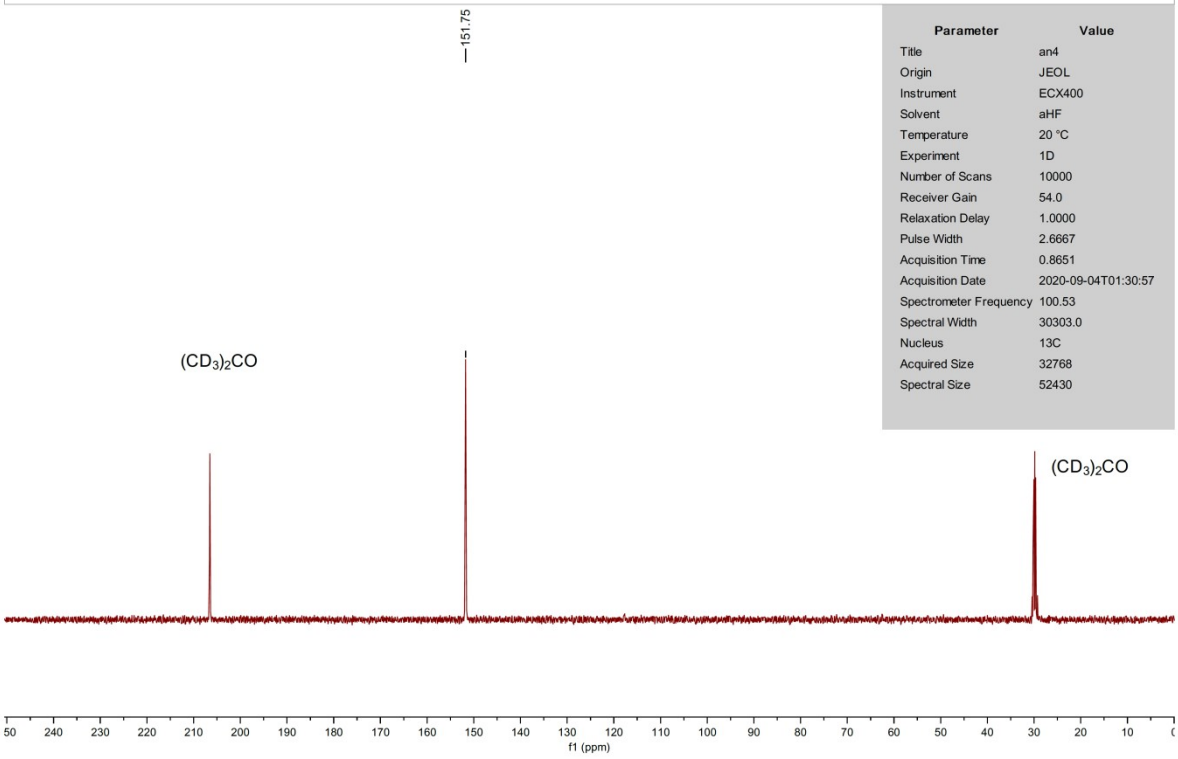

Parameter	Value
Title	an4
Origin	JEOL
Instrument	ECX400
Solvent	aHF
Temperature	20 °C
Experiment	1D
Number of Scans	10000
Receiver Gain	54.0
Relaxation Delay	1.0000
Pulse Width	2.6667
Acquisition Time	0.8651
Acquisition Date	2020-09-04T01:30:57
Spectrometer Frequency	100.53
Spectral Width	30303.0
Nucleus	13C
Acquired Size	32768
Spectral Size	52430

4.2 $[C_2N_3H_3O(OH)][SbF_6]$

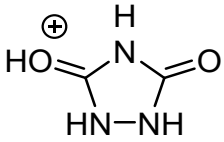

NMR (*a*HF, 25 ° C) (ppm): $\delta(^{14}N) = -246.67$; $\delta(^{13}C) = 151.60$.

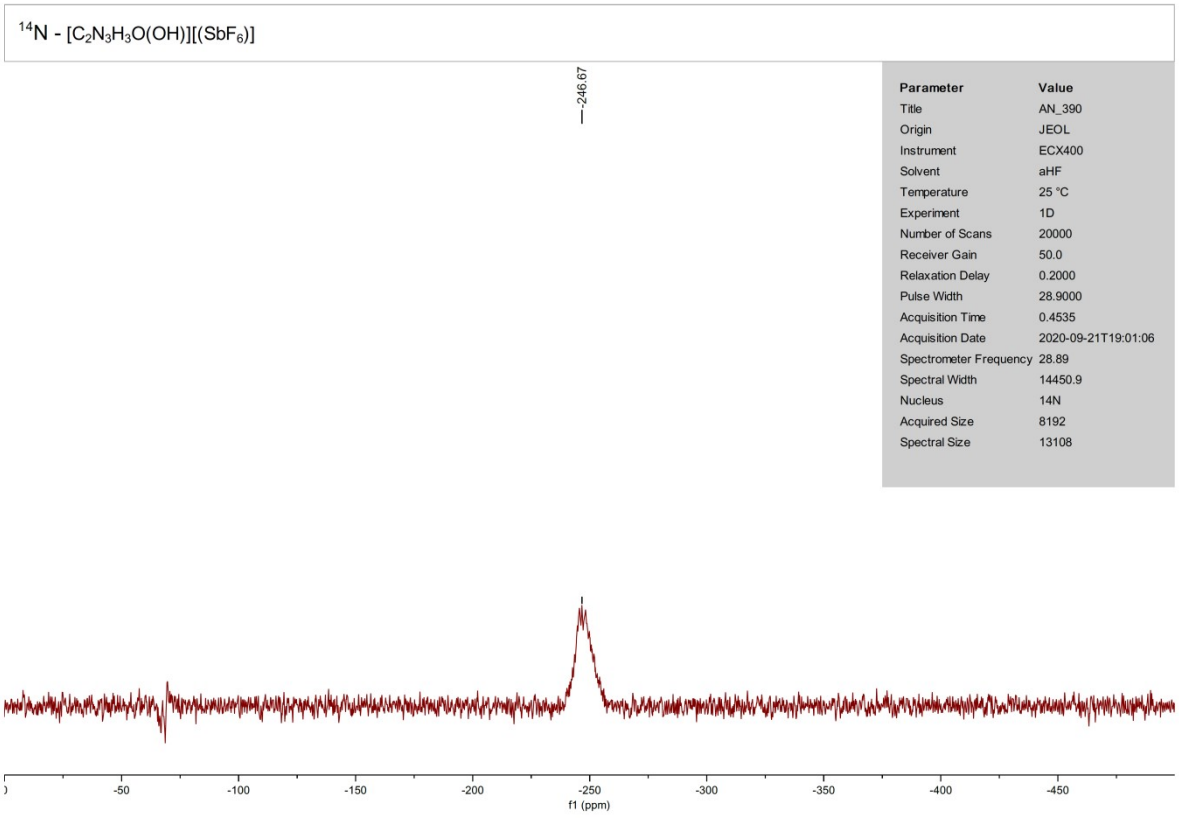

^{13}C - $[C_2N_3H_3O(OH)][(SbF_6)]$

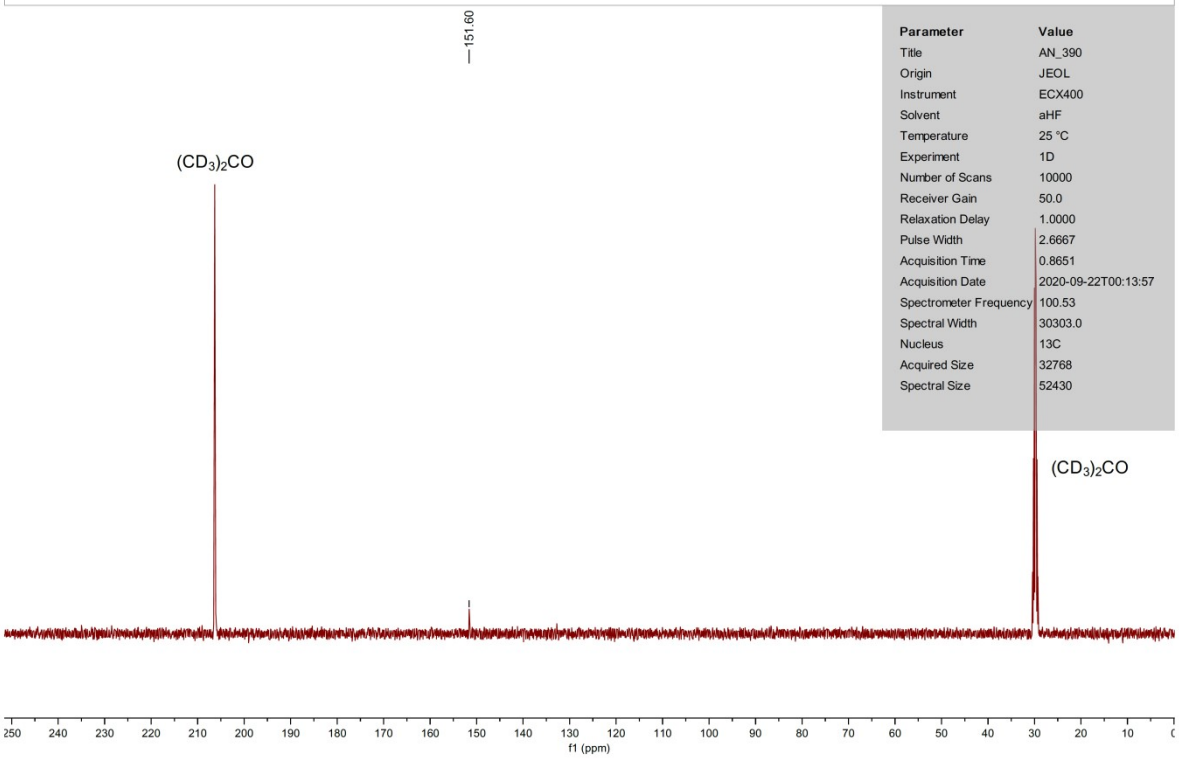

Parameter	Value
Title	AN_390
Origin	JEOL
Instrument	ECX400
Solvent	aHF
Temperature	25 °C
Experiment	1D
Number of Scans	10000
Receiver Gain	50.0
Relaxation Delay	1.0000
Pulse Width	2.6667
Acquisition Time	0.8651
Acquisition Date	2020-09-22T00:13:57
Spectrometer Frequency	100.53
Spectral Width	30303.0
Nucleus	13C
Acquired Size	32768
Spectral Size	52430

4.3 $[C_2N_3H_3(OH)_2][(SbF_6)_2]$

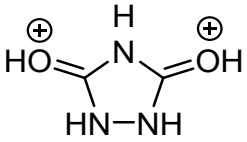

NMR (*a*HF, –40 to –30 ° C) (ppm): $\delta(^1H) = 10.09$ (OH^+); $\delta(^{13}C) = 151.12$.

NMR (*a*HF, 25 ° C) (ppm): $\delta(^1H) = 10.17$ (OH^+); $\delta(^{14}N) = -241.55$.

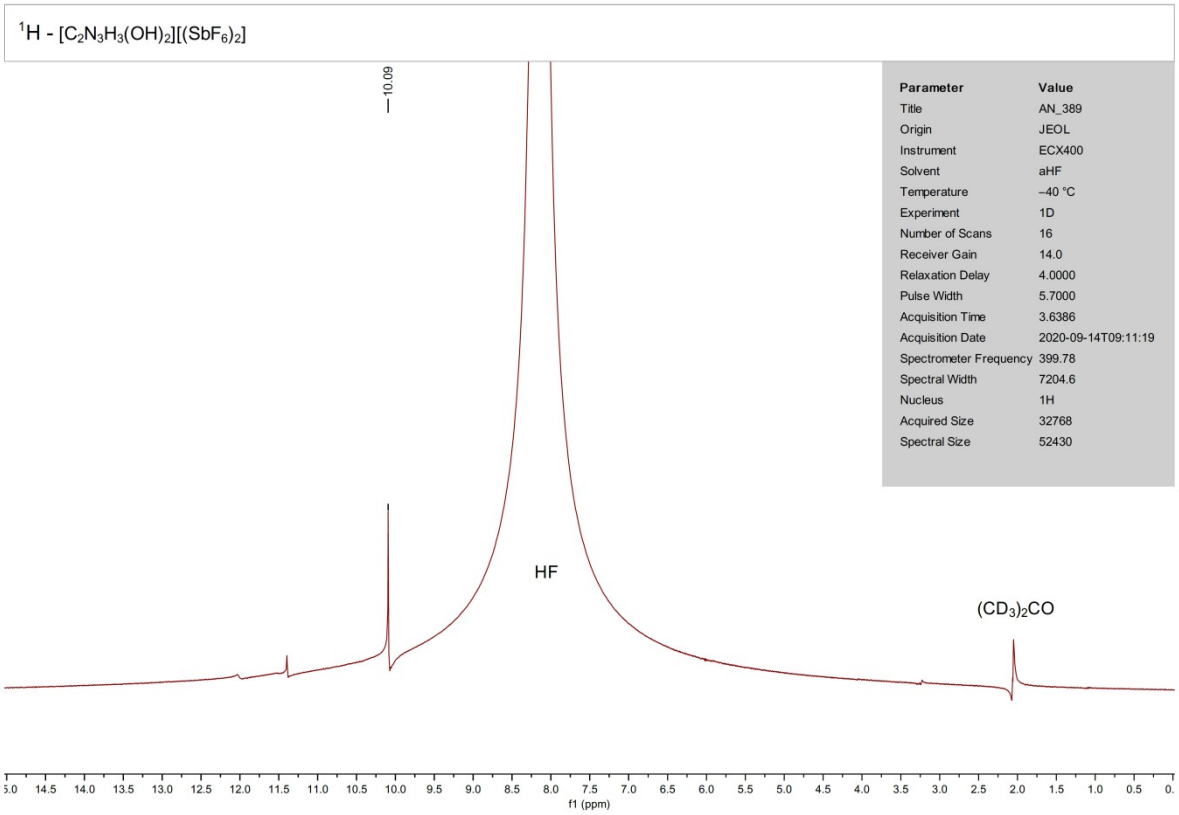

^{1}H - $[C_2N_3H_3(OH)_2][(SbF_6)_2]$

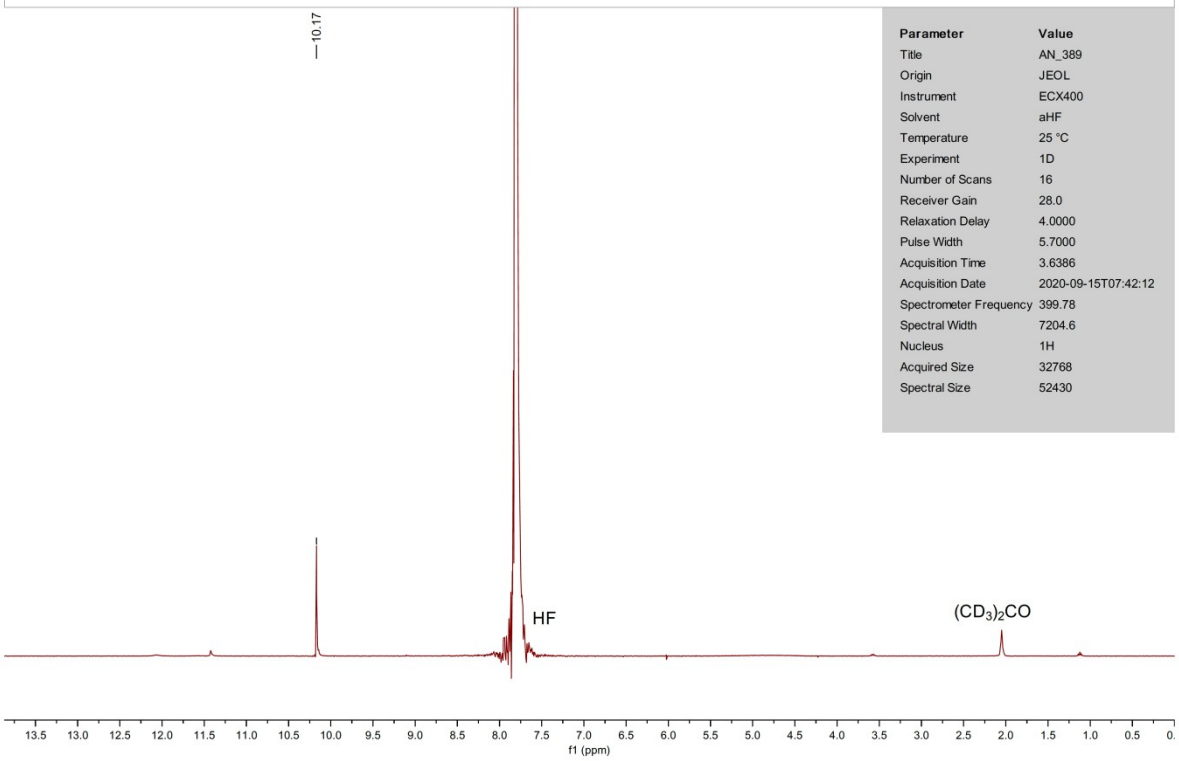

Parameter	Value
Title	AN_389
Origin	JEOL
Instrument	ECX400
Solvent	aHF
Temperature	25 °C
Experiment	1D
Number of Scans	16
Receiver Gain	28.0
Relaxation Delay	4.0000
Pulse Width	5.7000
Acquisition Time	3.6386
Acquisition Date	2020-09-15T07:42:12
Spectrometer Frequency	399.78
Spectral Width	7204.6
Nucleus	1H
Acquired Size	32768
Spectral Size	52430

^{13}C - $[C_2N_3H_3(OH)_2][(SbF_6)_2]$

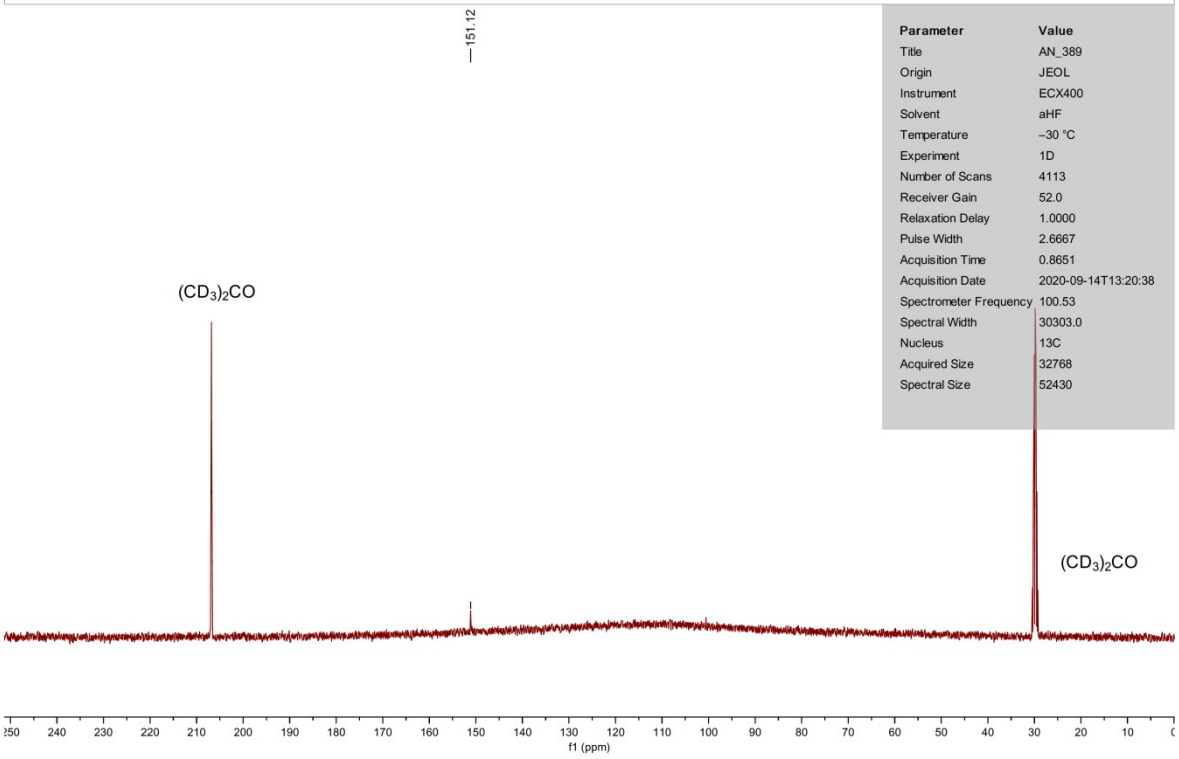

Parameter	Value
Title	AN_389
Origin	JEOL
Instrument	ECX400
Solvent	aHF
Temperature	–30 °C
Experiment	1D
Number of Scans	4113
Receiver Gain	52.0
Relaxation Delay	1.0000
Pulse Width	2.6667
Acquisition Time	0.8651
Acquisition Date	2020-09-14T13:20:38
Spectrometer Frequency	100.53
Spectral Width	30303.0
Nucleus	13C
Acquired Size	32768
Spectral Size	52430

^{14}N - $[C_2N_3H_3(OH)_2][(SbF_6)_2]$

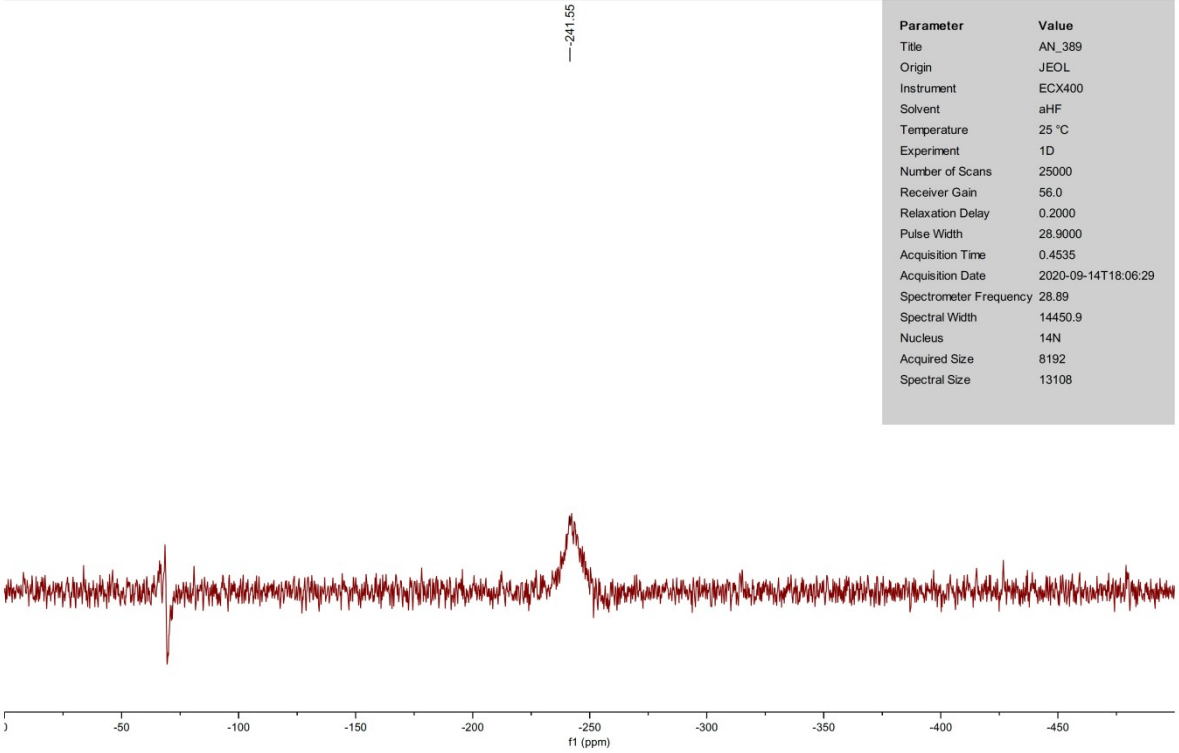

Parameter	Value
Title	AN_389
Origin	JEOL
Instrument	ECX400
Solvent	aHF
Temperature	25 °C
Experiment	1D
Number of Scans	25000
Receiver Gain	56.0
Relaxation Delay	0.2000
Pulse Width	28.9000
Acquisition Time	0.4535
Acquisition Date	2020-09-14T18:06:29
Spectrometer Frequency	28.89
Spectral Width	14450.9
Nucleus	14N
Acquired Size	8192
Spectral Size	13108

5.Quantum chemical calculations

5.1 Urazole

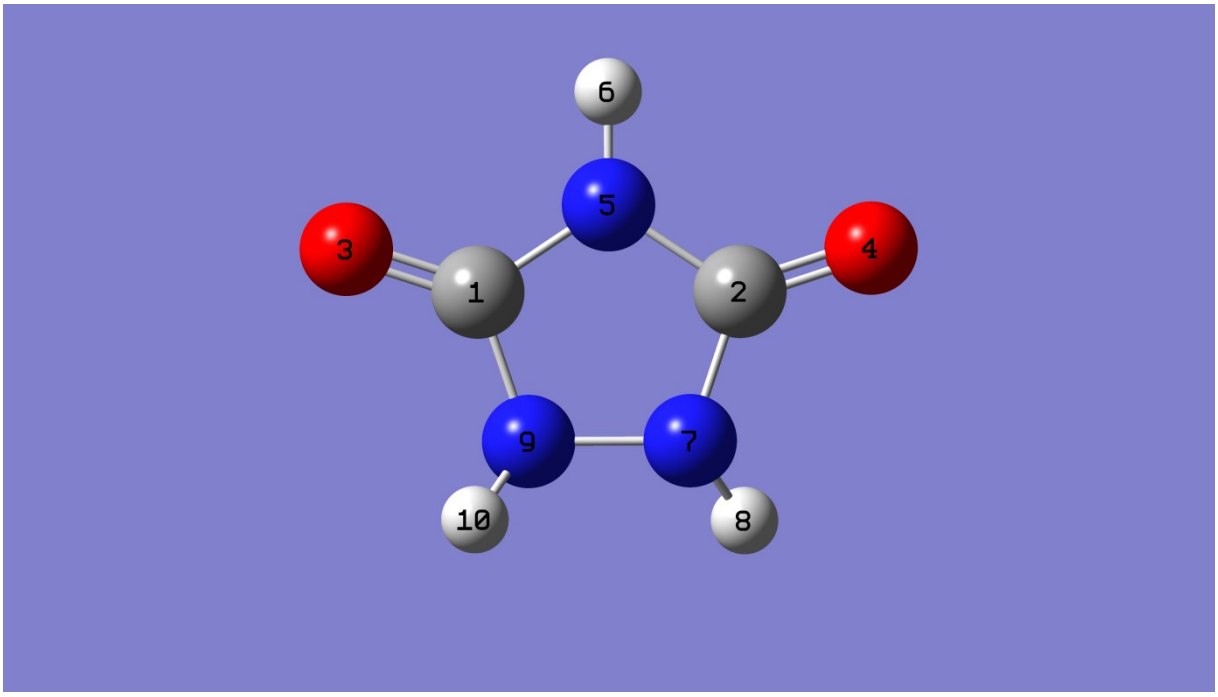

Figure 11: Optimized structure of urazole.

E(RB3LYP) = -392.721057950 Hartree

Standard orientation:

Center Number	Atomic Number	Atomic Type	Coordinates (Angstroms) X	Y	Z
1	6	0	-1.164644	-0.179483	0.029597
2	6	0	1.164643	-0.179478	-0.029562
3	8	0	-2.336473	-0.561909	-0.012535
4	8	0	2.336472	-0.561930	0.012389
5	7	0	-0.000023	-0.952382	0.000133
6	1	0	-0.000060	-1.957373	-0.000131

7	7	0	0.711826	1.147772	-0.104738
8	1	0	1.228523	1.849621	0.403437
9	7	0	-0.711816	1.147852	0.104813
10	1	0	-1.228358	1.849535	-0.403806

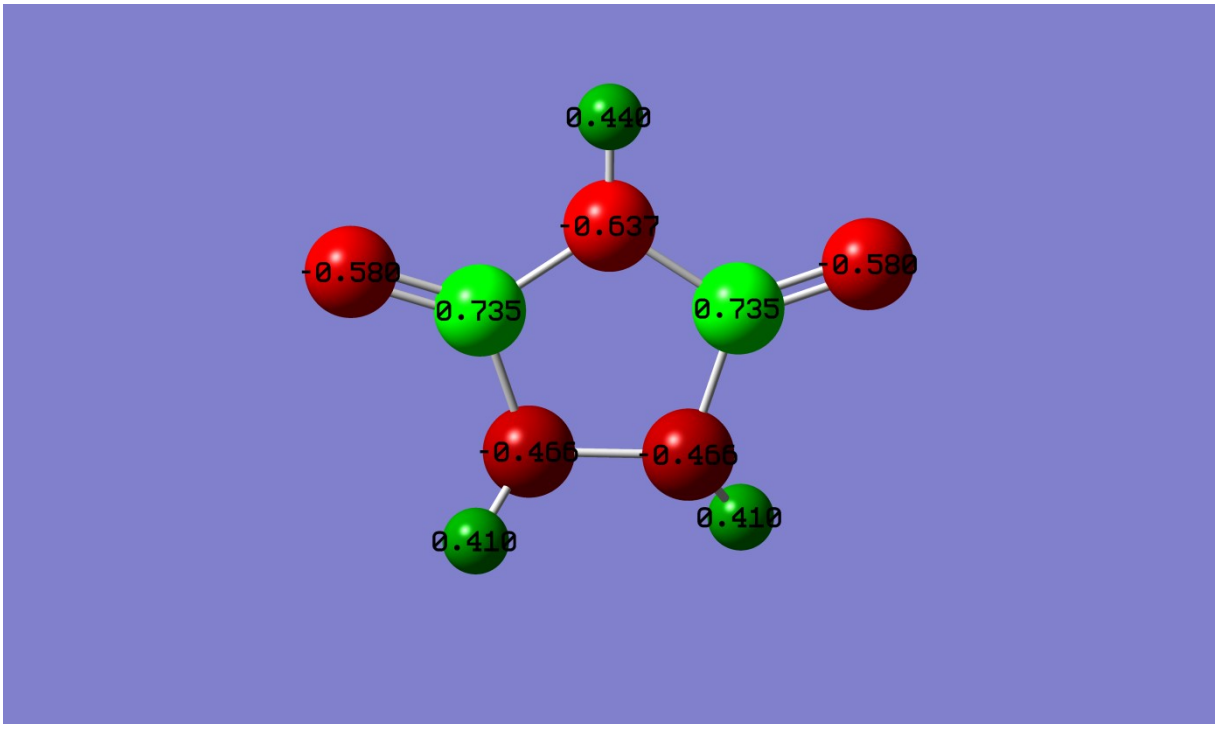

Figure 12: NPA charges of urazole.

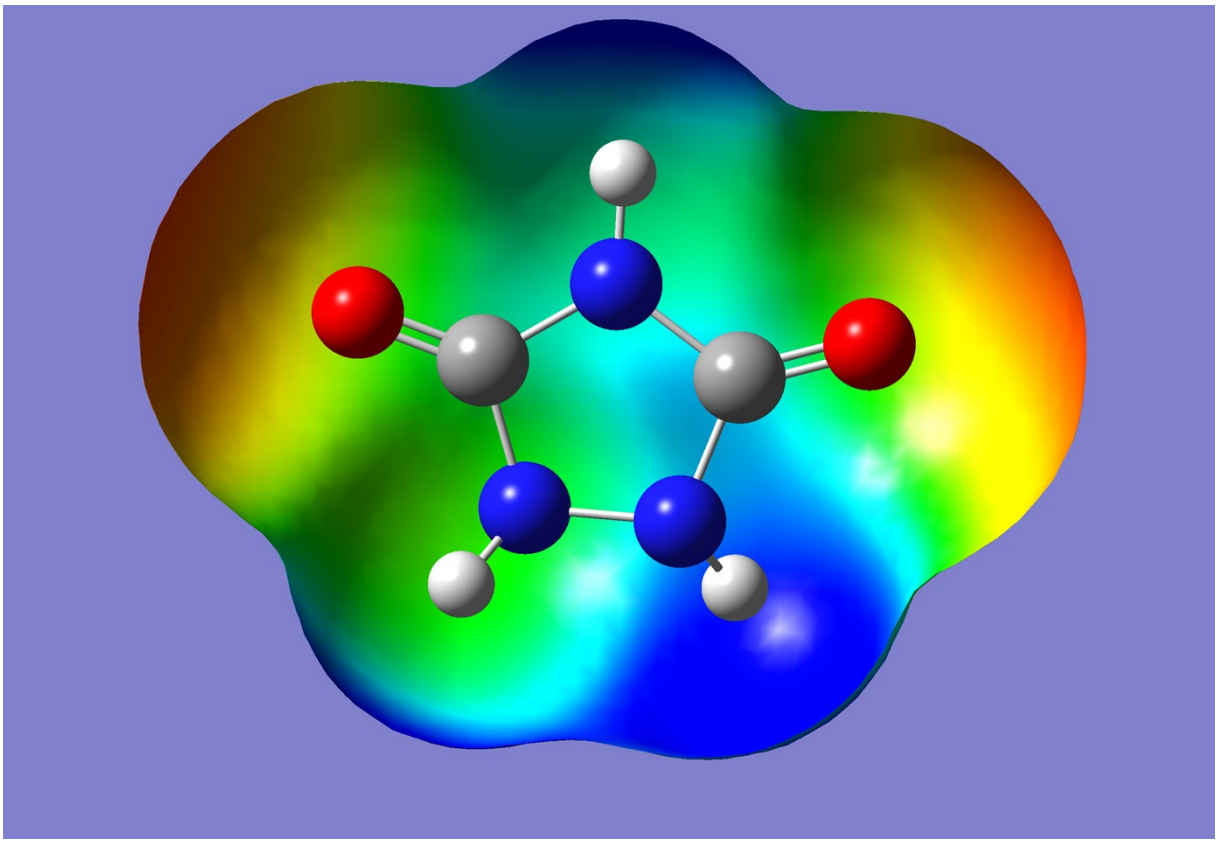

Figure 13: Molecular 0.0004 $bohr^{-3}$ 3D isosurfaces with mapped electrostatic potential of urazole (color scale ranging from -0.05 a.u. [red] to 0.05 a.u. [blue]).

5.2 [$C_2N_3H_3O(OH)$]

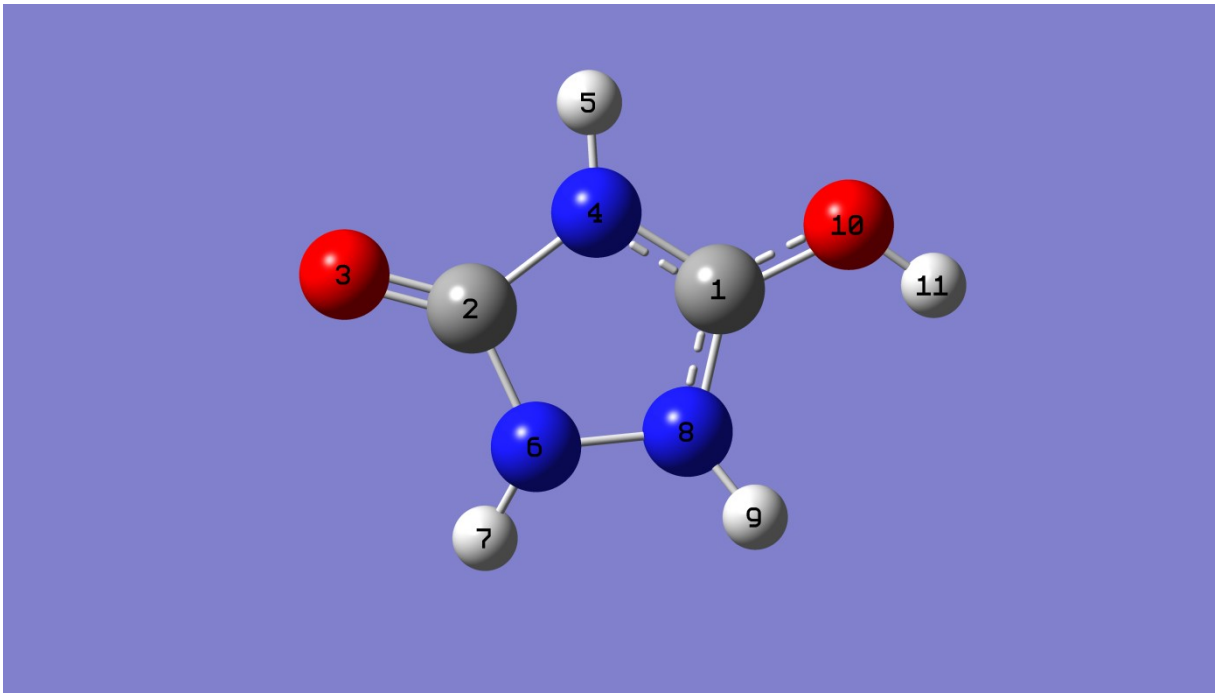

Figure 14: Optimized structure of [$C_2N_3H_3O(OH)$].

E(RB3LYP) = -393.037872928 Hartree

Standard orientation:

Center Number	Atomic Number	Atomic Type	Coordinates (Angstroms) X	Y	Z
1	6	0	1.053210	-0.123628	0.014108
2	6	0	-1.239565	-0.182968	-0.012475
3	8	0	-2.373394	-0.610105	0.013912
4	7	0	-0.008327	-0.940175	-0.009509
5	1	0	0.031146	-1.950377	0.011321
6	7	0	-0.782591	1.140740	-0.064120
7	1	0	-1.307821	1.935941	0.270947
8	7	0	0.628259	1.147241	0.036081

9	1	0	1.153562	1.986428	-0.161648
10	8	0	2.293022	-0.591255	-0.008280
11	1	0	3.022831	0.043829	0.087361

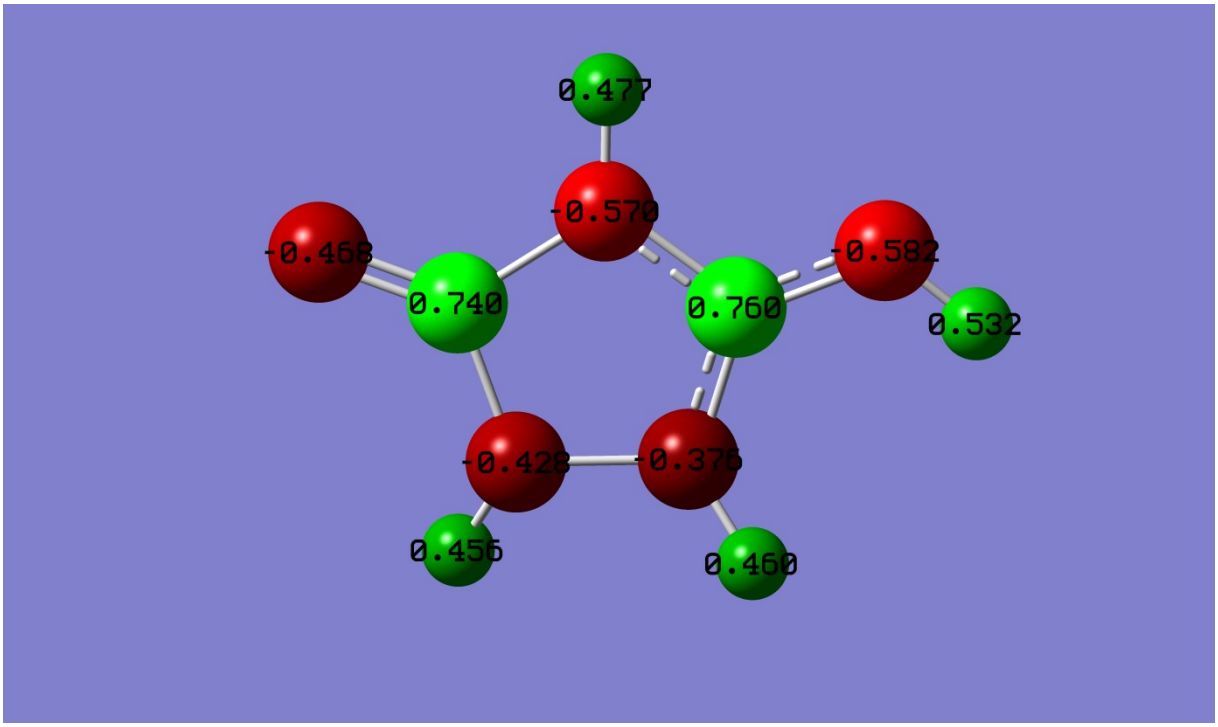

Figure 15: NPA charges of $[C_2N_3H_3O(OH)]$.

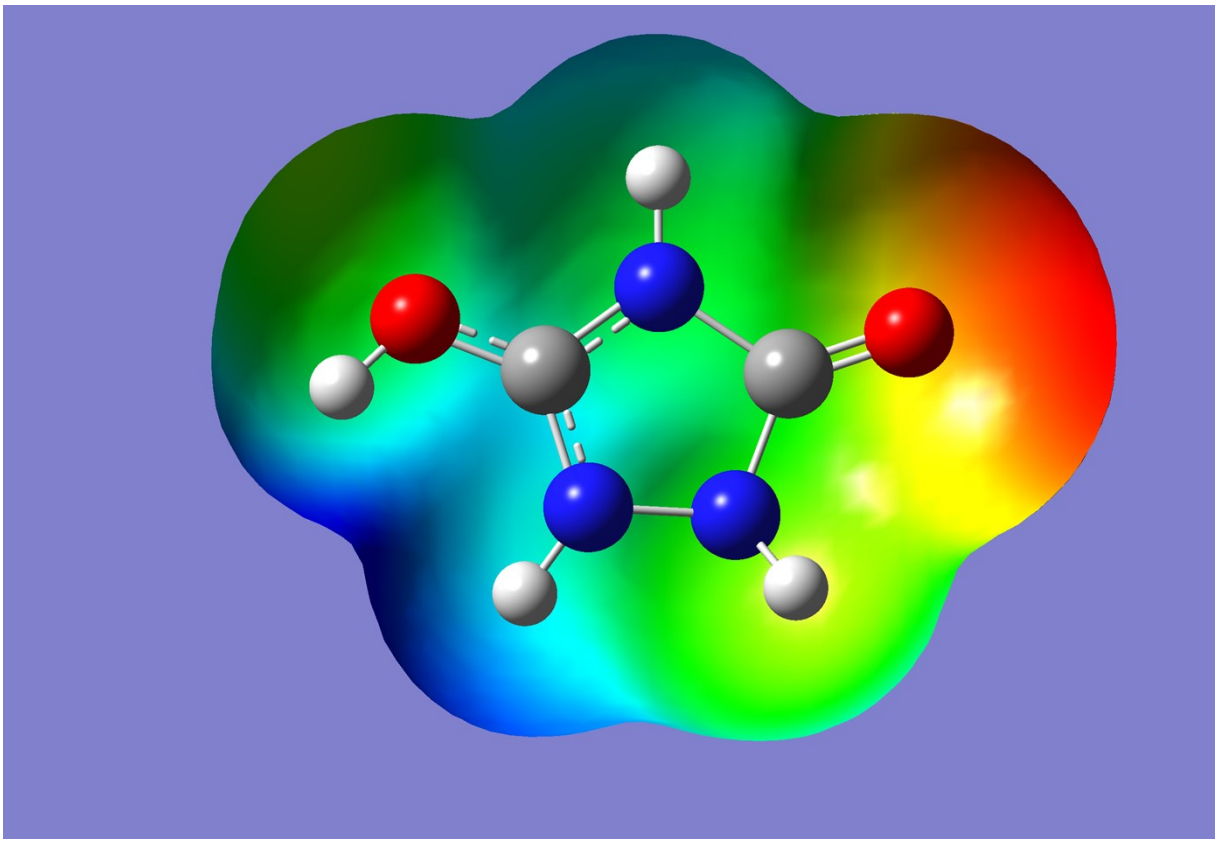

Figure 16: Molecular 0.0004 $bohr^{-3}$ 3D isosurfaces with mapped electrostatic potential of $[C_2N_3H_3O(OH)]$ (color scale ranging from 0.07 a.u. [red] to 0.24 a.u. [blue]).

5.3 [$C_2N_3H_3(OH)_2$]

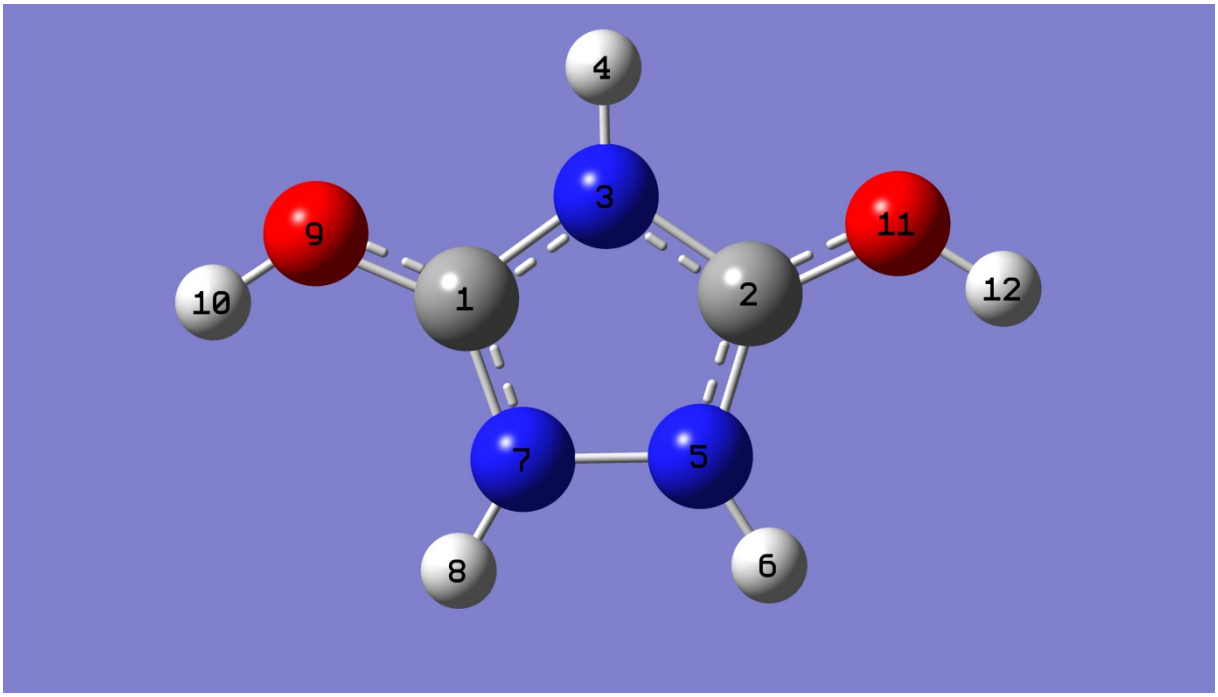

Figure 17: Optimized structure of [$C_2N_3H_3(OH)_2$].

E(RB3LYP) = -393.196301560 Hartree

Standard orientation:

Center Number	Atomic Number	Atomic Type	Coordinates (Angstroms) X	Y	Z
1	6	0	-1.121230	-0.116805	0.000012
2	6	0	1.121244	-0.116701	-0.000076
3	7	0	0.000047	-0.905603	0.000038
4	1	0	0.000173	-1.925780	0.000115
5	7	0	0.701470	1.161503	-0.000053
6	1	0	1.228036	2.032093	0.000609
7	7	0	-0.701547	1.161476	0.000099
8	1	0	-1.228171	2.032027	-0.000524

9	8	0	-2.301321	-0.651002	0.000035
10	1	0	-3.125271	-0.121590	-0.000443
11	8	0	2.301326	-0.650966	0.000005
12	1	0	3.125313	-0.121596	-0.000278

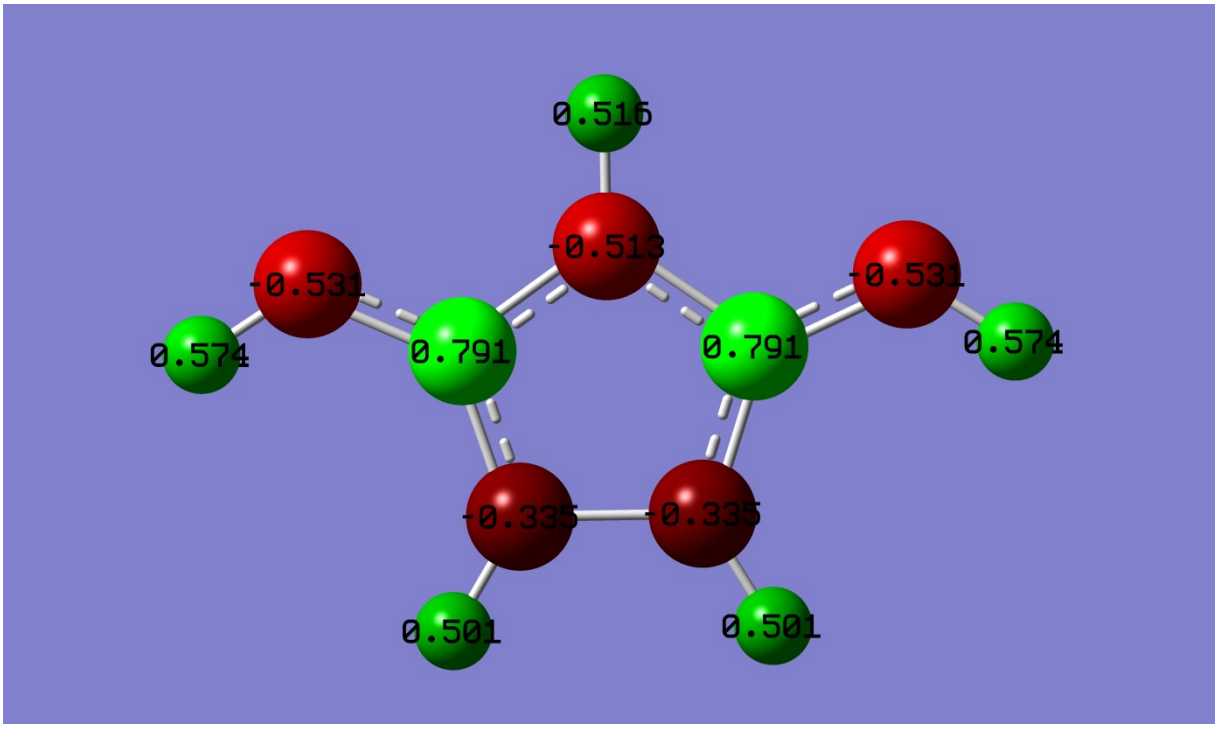

Figure 18: NPA charges of $[C_2N_3H_3(OH)_2]$.

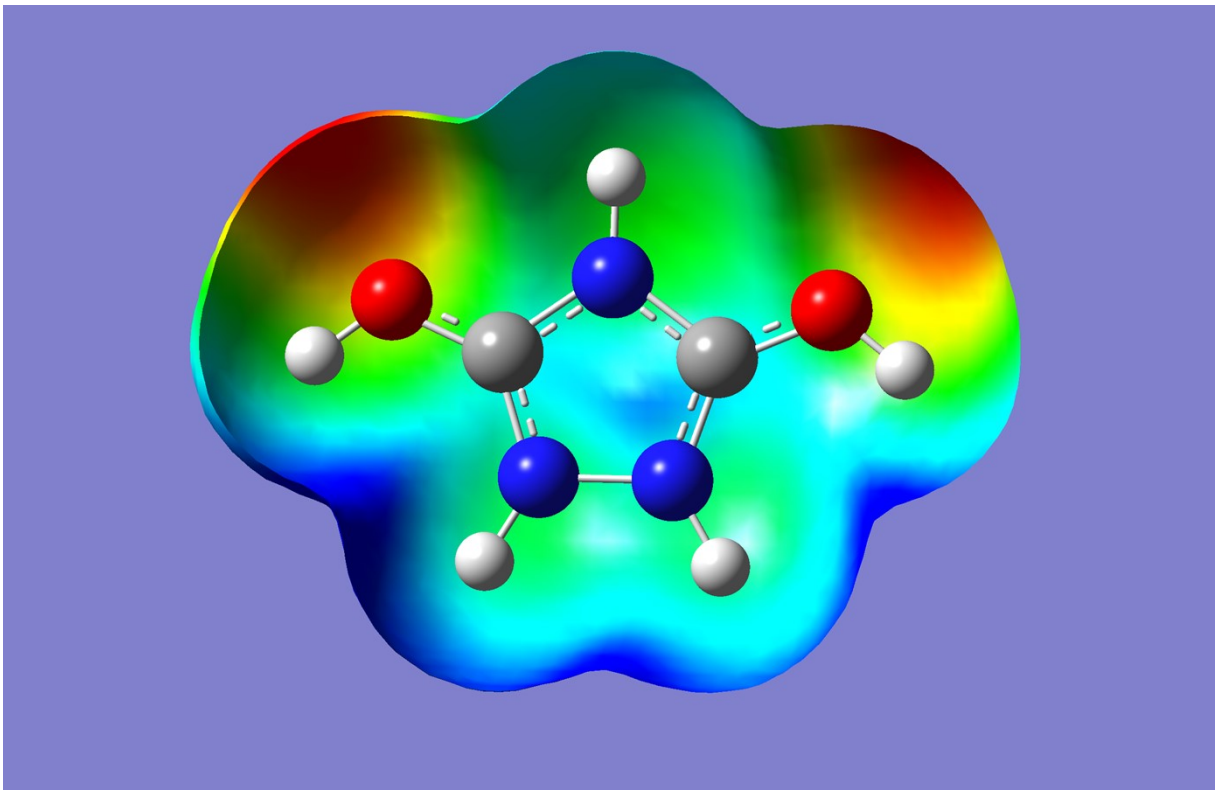

Figure 19: Molecular 0.0004 $bohr^{-3}$ 3D isosurfaces with mapped electrostatic potential of $[C_2N_3H_3(OH)_2]$ (color scale ranging from 0.26 a.u. [red] to 0.38 a.u. [blue]).

5.4 NPA charges

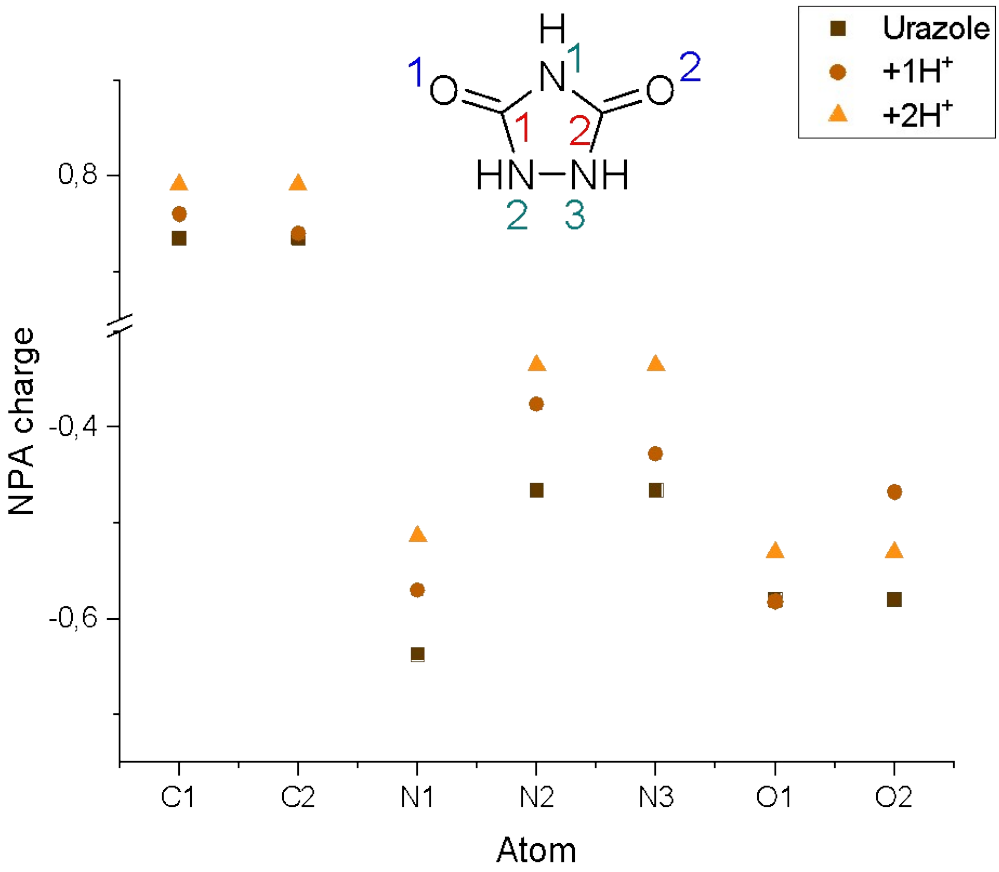

Figure 20: NPA charges of urazole and its protonated derivatives.

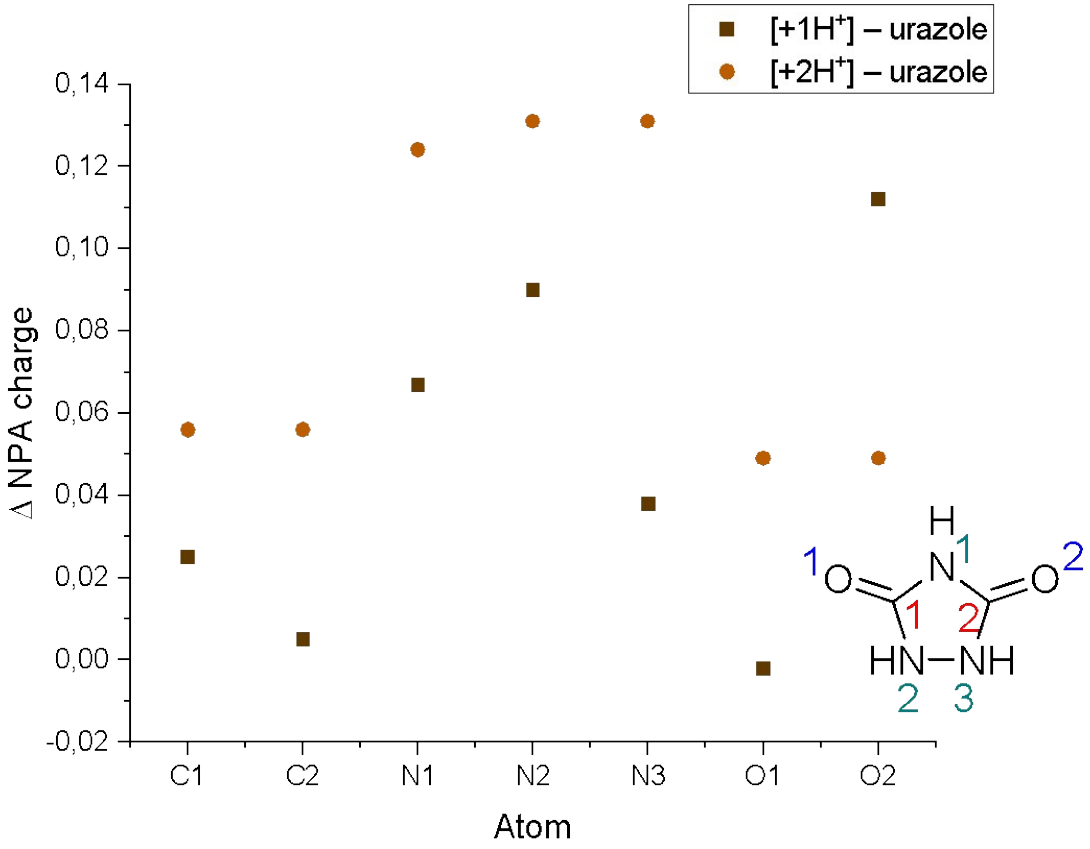

Figure 21: Difference in NPA charges of the respective protonated species vs urazole.

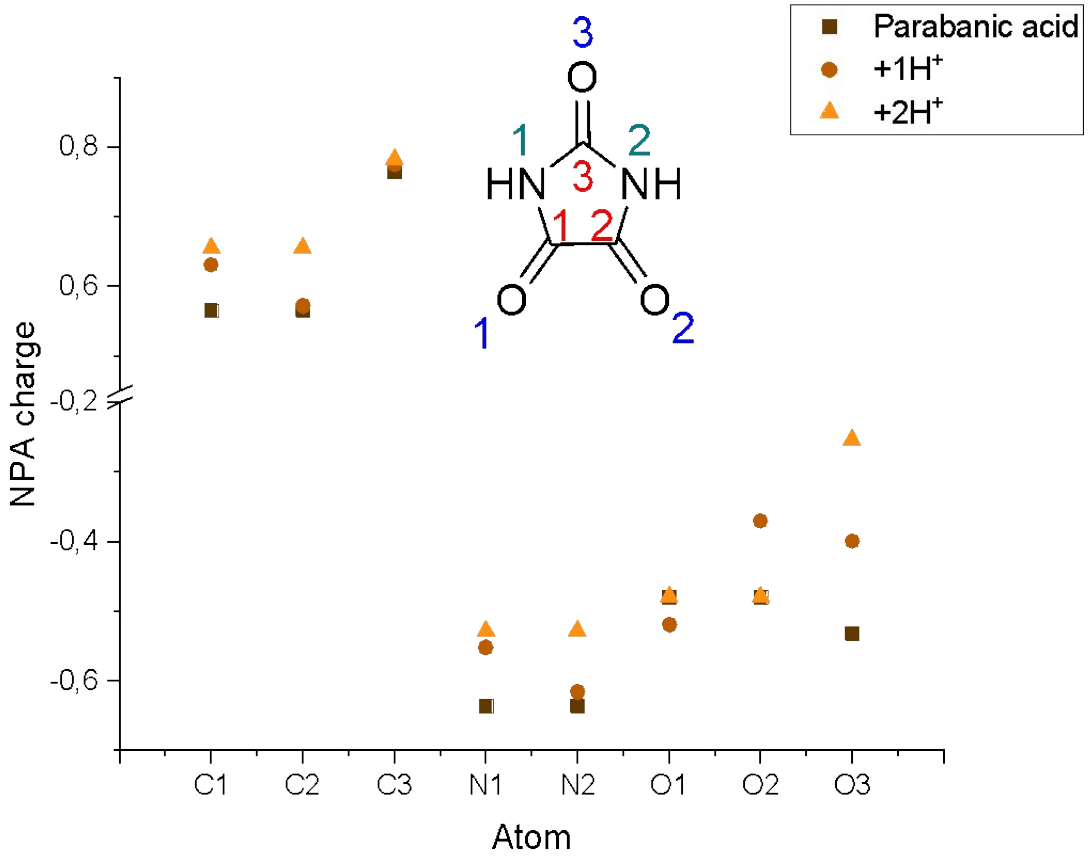

Figure 22: NPA charges of parabanic acid and its protonated derivatives.

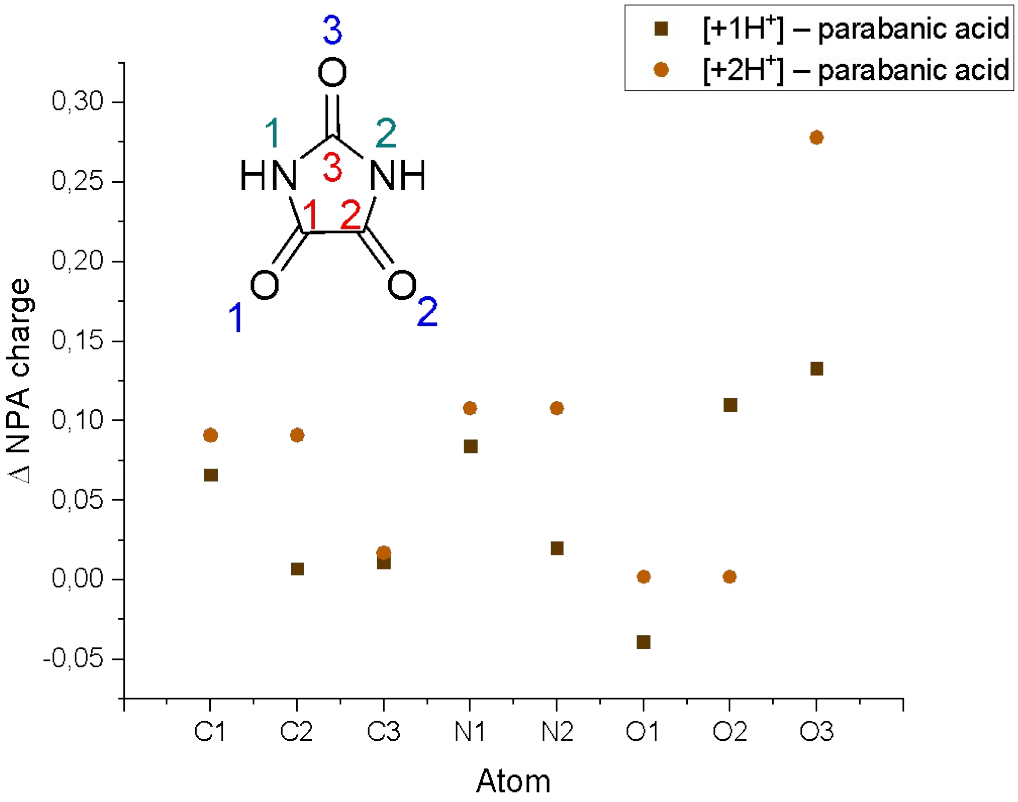

Figure 23: Difference in NPA charges of the respective protonated species vs parabanic acid.

6. Literature

[1] *MestReNova 12.0.2*; Mestrelab Research S.L., **2018**.

[2] Rigaku Oxford Diffraction, CrysAlisPro Software System, *Version 1.171.38.46*, Rigaku Corporation, Oxford, UK, **2015**.

[3] G. M. Sheldrick, *Acta Crystallogr. A* **2015**, *71*, 3. DOI: 10.1107/S2053273314026370.

[4] G. M. Sheldrick, *Acta Crystallogr. C* **2015**, *71*, 3. DOI: 10.1107/S2053229614024218.

[5] L. J. Farrugia, *J. Appl. Crystallogr.* **1999**, *32*, 837. DOI: 10.1107/S0021889899006020.

[6] A. L. Spek, *J. Appl. Crystallogr.* **2003**, *36*, 7. DOI: 10.1107/S0021889802022112.

[7] *SCALE3 ABSPACK*, *An Oxford Diffraction Program*, Oxford Diffraction Ltd, UK, **2005**.

[8] *Mercury 2020.2.0 (Build 290188)*, CCDC, **2020.**

[9] *Gaussian 16,* M. J. Frisch, G. W. Trucks, H. B. Schlegel, G. E. Scuseria, M. A. Robb, J. R. Cheeseman, G. Scalmani, V. Barone, G. A. Petersson, H. Nakatsuji, X. Li, M. Caricato, A. V. Marenich, J. Bloino, B. G. Janesko, R. Gomperts, B. Mennucci, H. P. Hratchian, J. V. Ortiz, A. F. Izmaylov, J. L. Sonnenberg, D. Williams-Young, F. Ding, F. Lipparini, F. Egidi, J. Goings, B. Peng, A. Petrone, T. Henderson, D. Ranasinghe, V. G. Zakrzewski, J. Gao, N. Rega, G. Zheng, W. Liang, M. Hada, M. Ehara, K. Toyota, R. Fukuda, J. Hasegawa, M. Ishida, T. Nakajima, Y. Honda, O. Kitao, H. Nakai, T. Vreven, K. Throssell, J. A. Montgomery, Jr., J. E. Peralta, F. Ogliaro, M. J. Bearpark, J. J. Heyd, E. N. Brothers, K. N. Kudin, V. N. Staroverov, T. A. Keith, R. Kobayashi, J. Normand, K. Raghavachari, A. P. Rendell, J. C. Burant, S. S. Iyengar, J. Tomasi, M. Cossi, J. M. Millam, M. Klene, C. Adamo, R. Cammi, J. W. Ochterski, R. L. Martin, K. Morokuma, O. Farkas, J. B. Foresman, and D. J. Fox, Gaussian, Inc., Wallingford CT, **2016**.

[10] *Gaussian 09,* M. J. Frisch, G. W. Trucks, H. B. Schlegel, G. E. Scuseria, M. A. Robb, J. R. Cheeseman, G. Scalmani, V. Barone, G. A. Petersson, H. Nakatsuji, X. Li, M. Caricato, A. Marenich, J. Bloino, B. G. Janesko, R. Gomperts, B. Mennucci, H. P. Hratchian, J. V. Ortiz, A. F. Izmaylov, J. L. Sonnenberg, D. Williams-Young, F. Ding, F. Lipparini, F. Egidi, J. Goings, B. Peng, A. Petrone, T. Henderson, D. Ranasinghe, V. G. Zakrzewski, J. Gao, N. Rega, G. Zheng, W. Liang, M. Hada, M. Ehara, K. Toyota, R. Fukuda, J. Hasegawa, M. Ishida, T. Nakajima, Y. Honda, O. Kitao, H. Nakai, T. Vreven, K. Throssell, J. A. Montgomery, Jr., J. E. Peralta, F. Ogliaro, M. Bearpark, J. J. Heyd, E. Brothers, K. N. Kudin, V. N. Staroverov, T. Keith, R. Kobayashi, J. Normand, K. Raghavachari, A. Rendell, J. C. Burant, S. S. Iyengar, J. Tomasi, M. Cossi, J. M. Millam, M. Klene, C. Adamo, R. Cammi, J. W. Ochterski, R. L. Martin, K. Morokuma, O. Farkas, J. B. Foresman, and D. J. Fox, Gaussian, Inc., Wallingford CT, **2016**.

[11] F. Belaj, *Acta Cryst.* **1992**, *48*, 1088–1090.